Targeting the Motion of Shikimate Kinase: Development of Competitive Inhibitors that Stabilize an Inactive Open Conformation of the Enzyme

Verónica Prado,[a] Emilio Lence,[a] María Maneiro,[a] Juan C. Vázquez-Ucha,[b] Alejandro Beceiro,[b] Paul Thompson,[c] Alastair R. Hawkins,[c] and Concepción González-Bello[a]*

[a]Centro Singular de Investigación en Química Biolóxica e Materiais Moleculares (CIQUS) and Departamento de Química Orgánica, Universidade de Santiago de Compostela, 15782 Santiago de Compostela, Spain.

[b]Servicio de Microbioloxía-INIBIC, Complexo Hospitalario Universitario A Coruña (CHUAC), 15006 A Coruña, Spain.

[c]Institute of Cell and Molecular Biosciences, Medical School, University of Newcastle upon Tyne, Newcastle upon Tyne NE2 4HH, UK.

CORRESPONDING AUTHOR ADDRESS. Dr. Concepción González-Bello, Centro Singular de Investigación en Química Biolóxica e Materiais Moleculares (CIQUS), Universidade de Santiago de Compostela, calle Jenaro de la Fuente s/n, 15782 Santiago de Compostela, Spain. FAX: +34 881 815704; Phone: +34 881 815726.

ABSTRACT

The large conformational changes observed by Molecular Dynamics simulation studies on the product release in the LID and shikimic acid binding (SB) domains of the shikimate kinase (SK) enzyme have been exploited in the development of reversible competitive inhibitors against SK from *M. tuberculosis* and *H. pylori*. This enzyme is is a recognized target for antibiotic drug discovery. The reported C5-substituted shikimic acid analogs interact with the dynamic apolar pocket that surrounds the C4 and C5 hydroxyl groups of the natural substrate, cause the opening of the LID and SB domains, and capture the essential arginine far from the ATP binding site as required for catalysis. The 3-nitrobenzyl **3e** and 5-benzothiophenyl derivatives **3i** proved to be the most potent inhibitors. An ester prodrug of **3i** was the most efficient derivative in achieving good *in vitro* activity against *H. pylori*, having a MIC value of 4 μg/mL.

INTRODUCTION

Antibiotics are probably the most successful drugs to be developed in the history of Medicine.[1] The discovery of penicillin in 1928 and the wide therapeutic arsenal developed thereafter have saved the lives of millions of people. Unfortunately, this enormous success was soon accompanied by the ever increasing emergence of drug resistance in bacteria, a problem that has become one of the most important public health issues of the early 21st century.[2–7] In a recent study it was demostrated that antibiotic resistance is a natural phenomenon that predates the golden age of antibiotic therapy, but the inappropriate and excessive use of these drugs in medicine, veterinary medicine and agriculture over the years has caused the antibiotic resistance problem to reach current levels.[8] It is therefore an urgent matter to develop novel and alternative therapies, to identify unexplored bacterial targets and to gain a detailed knowledge of the mechanism of action and binding determinants of those targets in order to develop effective inhibitors.

One of the most successful strategies to combat bacterial infections is based on the disruption of essential bacterial processes. However, most of the antibiotics in clinical use target a very small number of key bacterial functions and resistance to them is widespread and well known. Therefore, the search for unexplored bacterial functions appears to be a good option for the development of novel antimicrobial agents with a new mechanism of action. In this context, in recent years a great deal of attention has been devoted to the inhibition of the enzymes involved in the shikimic acid pathway, in which chorismic acid is synthesized.[9,10] This compound is the precursor of aromatic amino acids and other metabolites, including folates, ubiquinone and vitamins E and K. The fact that the enzymes involved in this pathway are essential in certain important microorganisms but absent in mammals makes them attractive targets for the development of antimicrobial agents.[11] Our recent work has focused on the development of inhibitors that target the fifth enzyme of the shikimic acid pathway, namely shikimate kinase (SK, EC 2.7.1.71, *aroK* gene).[9] SK is considered to be an attractive target for relevant pathogenic bacteria such as *Mycobacterium tuberculosis*, which is

responsible for tuberculosis, *Helicobacter pylori*, which is the causative agent of gastric and duodenal ulcers and has also been classified as a type I carcinogen, and *Pseudomonas aeruginosa*, which is one of the most common pathogens in healthcare-associated infections and represents 13% of multidrug-resistant strains to nearly all antibiotics. This enzyme is also essential in *Acinetobacter baylyi*, *Escherichia coli*, *Haemophilus influenza*, *Campylobacter jejuni* and *Francisella novicida*.[12] SK would therefore be an attractive target for the development of new drugs against several important bacterial diseases. Diverse compounds that target the SK enzyme have been discovered by screening (Figure 1). For example, Simithy *et al.*[13] used LC-MS and a library of about 400 antimycobacterial compounds, to identify several compounds with IC50 values in the micromolar range that inhibit SK from *M. tuberculosis* (*Mt*-SK). Moreover, Han *et al.*[14] discovered by high-throughput screening of a library of about 3000 compounds two inhibitors of SK from *Helicobacter pylori* (*Hp*-SK) with IC50 values also in the micromolar range.

SK catalyzes the stereospecific phosphorylation of the C3 hydroxyl group of shikimic acid (**1**) by transferring the γ-phosphate group of ATP to the hydroxyl group to provide shikimate 3-phosphate (**2**) and ADP (Scheme 1). NMR and computational studies have shown that the reaction catalyzed by SK involves a dissociative phosphoryl-transfer mechanism, in which a trigonal metaphosphate intermediate is formed first by cleavage of the γ O–P bond in ATP, followed by subsequent nucleophilic attack of the C3 hydroxyl group.[15] It was suggested that the rate-limiting step of the reaction would be the nucleophilic attack by the C3 hydroxyl group to the metaphosphate intermediate to afford a tetrahedral transition state. Moreover, based on the results of structural studies it was suggested that Asp33/Asp34 (in *H. pylori* and *M. tuberculosis*, respectively) would act as a general base to deprotonate the C3 hydroxyl group in **1** for nucleophilic attack.[16] SK is a magnesium-dependent enzyme that has two recognition centers, i.e., one for shikimic acid (**1**) and another for the cofactor (ATP), with different key interactions in both cases. SK has three domains: (1) the CORE domain that contains five stranded parallel β-sheets and the P-loop, which forms the

binding site for ATP and ADP; (2) the LID domain, which closes over the active site and has residues that are essential for the binding of ATP and catalysis; and (3) the substrate binding (SB) domain, which is responsible for the recognition and binding of **1** (Figure S1). The SK enzyme is amazingly designed to recognize an unstable conformation for a cyclohexene ring with two of the three hydroxyl groups in an axial arrangement. By forcing the diaxial disposition of the C4 and C5 hydroxyl groups, the enzyme controls the equatorial disposition of the C3 hydroxyl group and allows its selective phosphorylation. The available crystal structures show that shikimic acid (**1**) is anchored to the active site (SB domain) by a salt bridge with a conserved arginine (Arg132/Arg136 in *H. pylori* and *M. tuberculosis*, respectively), a double hydrogen bond between the side chain of a conserved aspartate (Asp33/Asp34 in *H. pylori* and *M. tuberculosis*, respectively) and the C3 and C4 hydroxyl groups, and a hydrogen bond between the C3 hydroxyl group and the NH main chain amide of a conserved glycine (Gly81/Gly80 in *H. pylori* and *M. tuberculosis*, respectively).[16,17] In addition, the C4 hydroxyl group is also fixed in an axial arrangement by hydrogen bonding with a structural water molecule (WAT1), the position of which is frozen by three conserved residues (Glu60/Glu61, Arg57/Arg58 and Gly81/Gly80 in *H. pylori* and *M. tuberculosis*, respectively). The axial disposition of the C5 hydroxyl group is controlled by two water molecules that interact by hydrogen bonding with the residues located in the LID. The substrate is surrounded by an apolar pocket generated by several lipophilic residues located in α-helices α2, α3 and α5 (SB domain) in such a way that it is isolated from the solvent environment.

Structural and Molecular Dynamics (MD) simulation studies also revealed that there are three key structural factors for catalysis:[18] (1) a closed form of the LID domain that allows the appropriate disposition of ATP in the active site, which is controlled by a cation-π interaction with Arg107/Arg110, and the activation of the γ-phosphate of ATP by the guanidinium group of the essential arginine Arg116/Arg117 (*H. pylori* and *M. tuberculosis*, respectively); (2) a closed form of the SB domain in order to bring the substrates together for the phosphoryl-transfer reaction and to

isolate the substrate within an apolar cavity; and (3) a flexible LID and SB domain for product release, which is triggered by the essential arginine.[18]

Reasoning that closed forms of the LID and SB domains are required for catalysis, we decided to explore the possible inhibition of the SK enzyme by blocking the appropriate closed form of those domains. To this end, we report here the synthesis and inhibitory properties against *Mt*-SK and *Hp*-SK of several shikimic acid analogs, namely compounds **3**–**6**, that incorporate diverse aromatic moieties at the C5 hydroxyl group of shikimic acid (**1**) (Figure 2). The design of the reported inhibitors was based on: (1) the dynamic behavior of the SB and LID domains observed during product release by MD simulations studies; (2) the role and the type of residues located in the SB domain in order to achieve the interaction with this `dynamic apolar´ pocket; and (3) the crystal structure of E114A *Hp*-SK variant enzyme in complex with the naphthalene derivative **7** (PDB entry 3N2E, 2.53 Å) described by Cheng *et al.*[19] (Figure 3). This structure reveals that this aromatic ligand, which has an IC_{50} value of 4.9 μM against *Hp*-SK, prevents closure of the active site for catalysis by causing a large conformational change in the LID domain with the subsequent inappropriate disposition of the essential arginine. The shikimic acid derivatives described here incorporate diverse *O*-benzyl groups (compounds **3**), and 1,2,3-triazole groups (compounds **4**–**5**). In addition, considering that (3*S*)-3-aminoshikimic acid[18] proved to be a competitive reversible inhibitor of *Mt*-SK with a K_i of 65 μM, we also studied the effect of replacing the C3 hydroxyl group in the *O*-benzyl derivatives **3** by an amino group, namely compounds **6**. The binding modes of the reported compounds with the two SK enzymes were initially studied using GOLD 5.2[20] and then further analyzed by MD simulation studies. The results of inhibition studies, along with the computational data, allowed us to understand the binding differences between the two enzymes. These studies also reveal that the intrinsic motion of an enzyme is a key point to be considered in inhibitor design.

RESULTS AND DISCUSSION

In order to be selective for this kinase, and considering that the binding site for ATP and ADP, which contains the consensus sequence GXXXXGKT/S (with X being any residue), is rather conserved in many ATP- or GTP-binding proteins, we focused on the design of compounds that bind to the SB binding site. The starting point for the design of the reported compounds was the study of the structural changes required in the SB and LID binding domains for the release of shikimate-3-phosphate (**2**) from the active site. This study was carried out by analyzing the dynamic behavior of the SK/ADP/**2** complex and the results are discussed below.

Dynamic Behavior of SK Enzymes: Molecular Dynamics Simulation Studies – For the *Mt*-SK enzyme, we have shown previously that an opening of up to 10 Å of the SB domain and of up to 8 Å of the LID domain are required for product release (Figure 4).[18] Overall, *Mt*-SK undergoes opening of the SB and LID domains in a similar way to the movement of an accordion, which is surprising given that the SB domain is composed of three α-helices α2, α3 and α5. This opening allows a rapid conformational change of the product to its thermodynamically favorable conformation, i.e., with the C4 and C5 hydroxyl groups in a pseudo-equatorial disposition. This process is mainly carried out by three conserved arginines, specifically Arg117, Arg136, and Arg58. The essential arginine triggers the process by pulling on the phosphate group of the product, which in turn breaks the key interactions with the active site.

In order to evaluate the possible differences between the two SK enzymes in relation to the structural changes required for product release, MD simulation studies were also performed with *Hp*-SK (Figure 5). The dynamic behavior of *Hp*-SK/ADP/**2** was studied by using the enzyme geometries found in the crystal structures of *Hp*-SK (PDB code 3MUF[19]) in complex with ADP and shikimate-3-phosphate (**2**). The monomer of *Hp*-SK immersed in a truncated octahedron of water molecules obtained using the molecular mechanics force field AMBER was used.[21] The results from 50 ns of dynamic simulation showed significant differences between the two enzymes. In general, for the *Hp*-SK enzyme the release of **2** from the active site is a much slower process since it is not initiated until

around 7 ns of dynamic simulation and this process requires to be performed at 50 ºC. For the *Mt*-SK enzyme, a large motion of the SB domain was already observed after ~20 ps of dynamic simulation at 25 ºC.[18] Even bearing in mind that the computational time cannot be correlated with the velocity of an enzyme, this finding is consistant with the huge velocity differences observed experimentally between the two enzymes. Thus, under the same assay conditions, *Hp*-SK has a k_{cat} value that is 2500-fold lower than that for *Mt*-SK. More importantly, the motion of the SB domain is also different. Whereas for the *Mt*-SK enzyme a synchronous and large opening of the three α-helices α2 (~7 Å), α3 (~10 Å) and α5 (~6 Å) was observed (Figure 5B), which is reminiscent of the movement of an accordion, for the *Hp*-SK enzyme an asynchronous and more reduced opening was observed (Figures S2-S4). Thus, conformational changes were mainly focused on α-helices α5 (~4 Å) and α3 (~3 Å), which in both cases were less pronounced than in the *M. tuberculosis* enzyme (Figure 5B). An opening of only a ~2 Å was observed for the α-helix α2. In contrast, significant differences were not observed in the opening of the LID domain, which was very large in both cases (up to 10 Å). Overall, the LID undergoes a large opening as for *Mt*-SK and part of the SB domain twists to create an additional gap in this region. These findings suggest that the 'dynamic pocket' in the SB domain of *Hp*-SK would be smaller and distinct from that in *Mt*-SK. In both cases the three conserved arginines are responsible for removing the product from the active site through strong electrostatic interactions between their guanidinium groups and the phosphate group in **2**. In addition, for the *Hp*-SK enzyme the presence of an arginine in α-helix α3 (Arg45) instead of an alanine (Ala46) in *Mt*-SK, which is oriented towards the active site, allows this residue to also be involved in product release (Figures 5C–5G).

Analysis of the available crystal structures and the amino acid sequence of various SK enzymes reveals that the apolar pocket surrounding the C4 and C5 hydroxyl groups of the natural substrate (SB domain), which undergoes the aforementioned motion, is quite conserved (Figures S5 and 6). This pocket mainly involves the conserved residues Phe48/Phe49, Phe56/Phe57, Ile36/Ile37 and

Val44/Ile45 (in *H. pylori* and *M. tuberculosis*, respectively). In addition, further sealing from the bulk water is achieved by several apolar residues in the vicinity (for *Hp*-SK: Leu51, Leu42, Val40 and Ile47; for *Mt*-SK: Ile60 and Ile48) and this also prevents the entry of water from the environment. Reasoning that the incorporation of benzyl groups in the C5 position of shikimic acid (**1**) would allow favorable contacts to be established with the apolar residues within the pocket and would prevent the appropriate closure of the active site for catalysis, we decided to explore the possible inhibition of the SK enzyme by compounds **3**–**6**. A range of substituted benzene rings were incorporated. Docking studies suggested that *meta*-substituted derivatives would lead to a more favorable effect than the corresponding *para*-substituted ones as the group would be pointing towards the protein. In addition, considering that *Mt*-SK appears to be able to achieve a wider opening of the SB domain than *Hp*-SK, we also studied the effect of larger aromatic moieties (naphthalene, benzothiophene, indole), compounds **3h**–**3i** and **4**–**5**. Finally, the effect of replacing the C3 hydroxyl group in *O*-benzyl derivatives **3** by an amino group was also analyzed with compounds **6**.

Synthesis of Compounds 3 – The synthesis of *O*-benzyl shikimic acid derivatives **3** was carried out from the previously described alcohol **8**,[22] which is synthesized in two steps from commercially available shikimic acid (**1**) (Scheme 2). Alkylation of alcohol **8** with various benzyl bromide derivatives in the presence of sodium iodide and diisopropylethylamine at 150 ºC afforded benzyl ethers **9**. Removal of the acetal group in **9** with HCl followed by basic hydrolysis of the resulting esters **10** and, in some cases, subsequent protonation with Amberlite IR-120 (H^+) ion-exchange resin gave the *O*-benzyl shikimic acid derivatives **3** or their corresponding sodium salts. For compounds **9d** and **9f**, treatment with HCl directly afforded the corresponding acids **3d** and **3f**, respectively.

Synthesis of Compounds 4 and 5 – The triazole moiety in **4**–**5** was introduced by a copper(I)-catalyzed 1,3-dipolar cycloaddition between azide **14** and 3-phenyl-1-propyne or 3-phenoxy-1-propyne, respectively (Scheme 3). Azide **14**[23] was prepared in four steps from protected methyl

shikimate **11**[24] following a modified procedure. First, treatment of alcohol **11** with mesyl chloride in the presence of trimethylamine and subsequent acid hydrolysis of the acetal gave mesylate **12**. Treatment of diol **12** with sodium methoxide and methanol afforded epoxide **13**,[25] which was treated with sodium azide to give the desired azide **14**. The cycloaddition reaction regioselectively afforded the 4-substituted triazoles **15** and **16**. Basic hydrolysis of the resulting methyl esters **15** and **16** and protonation with an ion-exchange resin, led to the desired acids **4** and **5**.

Synthesis of Compounds 6h–i – The C3 amino group in compounds **6h** and **6i** was introduced by Mitsunobu reaction between diols **10h**–**i** and freshly prepared hydrazoic acid followed by reduction of the resulting azides (Scheme 4). Finally, basic hydrolysis of the amino methyl esters **17h**–**i** gave the desired amines **6h**–**i**.

Inhibitory Activity and Susceptibility Testing – The inhibitory properties of compounds **3**–**6** against both SK enzymes were tested. Enzyme activity was measured by UV monitoring of ADP formation by coupling the released ADP to the oxidation of NADH using pyruvate kinase (PK) and lactate dehydrogenase (LDH) as coupling enzymes. The disappearance of NADH by oxidation to NAD during PK-LDH activity was monitored at 340 nm. All of the compounds that were found not to be substrates for this enzyme were assayed in the presence of shikimic acid (**1**) and ATP for their inhibitory properties against *Mt*-SK and *Hp*-SK. All compounds proved to be reversible competitive inhibitors of both enzymes. The inhibition data (K_i), which were obtained from Dixon plots (1/v *vs* [I]), are provided in Table 1.

In general, the reported compounds proved to be more potent against *Hp*-SK than *Mt*-SK. Compounds **4**–**6** were found to have K_i values above the K_m (Table 1, entries 10–13). In contrast, compounds **3**, which bear *O*-benzyl groups, were the best inhibitors for both enzymes with K_i values below K_m in most cases (Table 1, entries 1–9). For *Hp*-SK, the latter compounds were found to have K_i values in the low micromolar or nanomolar range. The results show that the incorporation of

substituents in the *meta*-position of the benzene ring and the use of large aromatic rings enhances the inhibitory potency by up to 36-fold. The most potent inhibitor in series **3** was the 3-nitrobenzyl derivative **3e**, which gave K_i values of 0.46 μM and 10 μM against *Hp*-SK and *Mt*-SK, respectively (Table 1, entry 5). 5-Benzothiophenyl derivative **3i** was also potent, with a K_i value of 0.56 μM against *Hp*-SK. In view of the high inhibitory potency of the 3-nitrobenzyl derivative **3e** against both enzymes, the high K_i values obtained with the perfluoro derivative **3g** are surprising (Table 1, entry 7). Compounds **3i** and **3e** proved to inhibit more efficiently *Hp*-SK than previously reported ones.[19]

The *in vitro* anti-*Helicobacter pylori* activity of the most potent inhibitors of series **3**, compounds **3e** and **3i**, and compounds **4**–**6** was studied. Considering the high hydrophilicity of these compounds due to the presence of a carboxylate group, which is required for enzyme recognition by the conserved Arg132, their corresponding methyl ester prodrugs (compounds **10e**, **10i**, **15–16** and **17h-i**) were employed. We have previously used this strategy to achieve the internalization into mycobacterial cell of diverse reversible competitive inhibitors of the type II dehydroquinase, the third enzyme of the shikimic acid pathway.[26] In the latter case, the free acids also proved to have low *in vitro* activity. The agar dilution method was used to determine the Minimum Inhibitory Concentration (MICs, μg/mL) of the compounds, according to the standard method recommended by CLSI.[27] A *H. pylori* clinical isolate obtained from a biopsy of a patient of the Guadalajara Hospital (Guadalajara, Spain) was employed. MICs were defined as the lowest concentration of each compound that completely inhibited visible growth on plates. MIC assays were performed at least three times. The results are provided in Table 2. The methyl ester **10i**, which is the ester prodrug of the 5-benzothiophenyl derivative **3i** with a K_i value of 560 nM, proved to be the most potent with an MIC value of 4 μg/mL. Derivative **10e** proved to have a 32-fold higher MIC value, which might be due to the lower stability of the nitrobenzyl moiety *vs* the benzothiophenyl one. As expected, higher MICs values were obtained for methyl esters **15–16** and **17h-i**.

In an effort to obtain further details of the binding interactions responsible for the inhibitory activity, the binding modes of compounds **3**–**6** with *Mt*-SK and *Hp*-SK were studied. Molecular docking using GOLD 5.2[20] was initially carried out with diverse inactive open forms of the SK active site. The proposed binding modes were further analyzed by MD simulation studies and the results are discussed below.

Binding Mode – Diverse inactive open conformations of the two enzymes, which were obtained by MD simulation studies, were employed for docking studies. For the *Hp*-SK enzyme, the first 15 ns of the MD simulation of the *Hp*-SK products complex provided diverse poses of the LID and SB domains in the open conformation. However, for the *Mt*-SK enzyme, the MD simulation performed with the *Mt*-SK/ADP/**2** complex showed that as soon as the simulation starts large displacements in the positions of the conserved and essential active site residues occur. For instance, this is the case for the conserved Arg136, which is the key residue for carboxylate recognition in the substrate. Considering that under these circumstances the binding mode determined by GOLD might be quite unrealistic, diverse poses from the MD simulation of *Mt*-SK/ATP/(6*R*)-6-hydroxyshikimic acid were employed for docking studies (Figures 3C and 3D). The latter compound seemed to cause the opening of the SB domain (4 Å) due to a conformational change to the most stable conformation of a cyclohexene ring but without large displacements of the conserved arginines.[18]

In general, as one would expect from the incorporation of a large substituent in the C5 position of **1**, all of the ligands bind in the active site with the most stable conformation for a cyclohexene ring, i.e., with the C4 and C5 substituents in a pseudo-diequatorial disposition. The rigidity that the triazole moiety imparts to compounds **4** and **5** would disfavor their binding because the benzyl moiety would be more restricted in terms of finding the optimal conformation to achieve good binding with the apolar pocket – a situation that might explain their low inhibitory potency. The same limitation was observed with the incorporation of an amino group in the C3 position (compounds **6h** and **6i**). This group would cause the ligands to be in close contact with the γ-phosphate of ATP due to attractive

electrostatic interactions between the phosphate group and the protonated amino group of the ligands. Fortunately, *O*-benzyl derivatives **3** proved to bind in the active site of the two SK enzymes, with the aromatic moiety interacting with the apolar pocket of the SB domain as desired. The highest score solutions of the most potent inhibitors, specifically compound **3e** for *Mt*-SK and compounds **3e**, **3b**, and **3i** for *Hp*-SK, were further evaluated by MD simulation studies in order to assess the stability and therefore the reliability of the proposed binding mode. The results of the MD simulation studies (50 ns) show that the aforementioned complexes are stable as relevant differences were not observed in the position of the ligand during most of the simulation. Overall, our computational studies revealed that there are significant differences in the conformational changes caused by the ligands in the LID and SB domains based on the size of the aromatic moiety incorporated on the C5 hydroxyl group as well as the type of SK enzyme. The results of these studies are discussed below.

*O-Benzyl derivative **3e*** – The binding mode of the most potent inhibitor of the monobenzyl series for the two enzymes, namely the nitro derivative **3e**, proved to be significantly different in the active sites of *Mt*-SK (Figures 7A and 7D) and *Hp*-SK (Figures 7B and 7E). In the case of *Mt*-SK, the incorporation of the 3-nitrobenzyl moiety at the C5 position of **1** would cause the opening of the LID domain (9 Å) and α-helix α3 of the SB domain (5 Å). This aromatic moiety would cause a large conformational change in the position of the essential arginine and a reduction in the flexibility of the LID and SB domains through a set of favorable lipophilic interactions with apolar residues of these domains. The 3-nitrobenzyl moiety would be trapped between the essential residues Phe49 and Arg117 by establishing π-π stacking and cation-π interactions, respectively. The interaction with the essential arginine seems to be crucial to enhance the binding affinity of the ligands in the active site and therefore their inhibitory potency. The nitro group would be pointing towards α-helix α3. In this arrangement the benzyl group would interact with the side chains of Ile45 and Phe57 (α-helix α3) and with the side chain of Val116 and the carbon chain of Arg117 of the LID. In contrast, for the *Hp*-SK enzyme the 3-nitrobenzyl moiety in **3e** would stabilize an open conformation of the SB domain

(mainly α-helices α2 and α5) by interaction with the apolar pocket between α-helices α3 and α5, instead of α-helix α3 (Figures 7B and 7E). Significant changes were not observed in the position of the essential arginine and the LID domain. The 3-nitrobenzyl moiety would now be located between the essential Phe48 and the carbon side chain of the conserved residue Glu53, with the nitro group pointing towards the LID domain instead of towards α-helix α3. In this arrangement the benzyl group would establish π-π stacking interactions with Phe48 and lipophilic interactions with the side chains of Ile47, Leu51 and Glu53 (carbon chain). Moreover, the C5 CH group in **3e** would interact with the side chain of Phe56 and the aromatic ring and the C6 methylene group would contact the side chain of Leu118, which is located in the LID.

*O-Benzyl derivative **3b*** – The introduction of a large and apolar methoxy group in the benzyl ring, namely compound **3b**, which had a K_i of 1 μM against *Hp*-SK, would also stabilize an open conformation of the LID domain (Figures 7C and 7H). By establishing favorable lipophilic interactions with Leu118, the ligand is more embedded in the active site and this allows apolar interactions between the side chain of Met10 and the C3 and C4 CH bonds of the cyclohexene ring. Moreover, this compound also locates its benzyl group in the apolar pocket between α-helices α3 and α5 but causes the opening of α-helix α5 only. The main difference with compound **3e** with respect to the lipophilic interactions with side chain residues Ile47, Phe56 and Phe48 is the lack of a π-π stacking interaction between the benzyl moiety in **3b** and the essential Phe48, which might account for the lower inhibitory potency.

In general, the results of our MD simulation studies revealed that the substituent in the *meta*-position in **3** would prefer to point towards the LID domain in the two SK enzymes. The exception to this trend is the 3-nitrobenzyl derivative **3e** when it binds with *Mt*-SK. In this case, the essential Arg117 seems to select the opposite arrangement to establish a strong cation-π interaction with the ring – an interaction that was not observed in the other analogs of the series or with the *Hp*-SK enzyme. In

order to obtain further evidence for this trend, MD simulation studies with the 3-nitro derivative **3e** and the 3-methoxybenzyl derivative **3b** were carried out with the two possible orientations of the substituent, i.e., pointing toward the LID or the SB domains. The binding free energies of these ligands were calculated using the MM/PBSA[28] approach in explicit water (generalized Born, GB) as implemented in Amber. For *Mt*-SK, the calculated binding energy of the 3-nitrobenzyl derivative **3e** when the nitro group is pointing towards the SB domain is –23.1 kcal lower than for the opposite pose. In addition, the 3-methoxybenzyl derivative **3b** arranged with the methoxy group pointing towards the SB domain undergoes a rotation of 180° during the 50 ns of simulation to give the opposite pose. For *Hp*-SK, the calculated binding energy of **3b** with the methoxy group pointing towards the LID domain is –16.7 kcal lower than that for the opposite pose. A less marked difference between the two poses was obtained for the nitro compound **3e** (1.9 kcal). However, the aforementioned binding mode provides a more stable complex during the whole simulation.

*O-Benzyl derivative **3i*** – The benzothiophene derivative **3i**, which had a K_i value of 560 nM against *Hp*-SK, was predicted to have a similar binding mode to the 3-methoxy derivative **3b** (Figures 7G and 7H). Thus, this compound would also stabilize an open conformation of the LID (5 Å) and the SB (3 Å) domains. As shown in Figure 7I, although both ligands interact with the same residues, the arrangement and rigidity of the benzothiophene ring would probably enhance the binding, which might account for the 2-fold higher inhibitory potency.

CONCLUSIONS AND FINAL REMARKS

Several C5-substituted shikimic acid analogs, compounds **3**–**6**, have been synthesized and tested against SK from *M. tuberculosis* and *H. pylori*, an essential enzyme in bacteria. These compounds were designed to explore the possible inhibition of the SK enzyme by blocking the appropriate closed form for catalysis. The two enzymes were found to undergo large conformational changes for product release in the LID and SB domains but they were particularly distinct in the latter domain.

Specifically, the ‘dynamic apolar pocket’ that isolates the substrate for catalysis and involves a quite conserved region of α-helices α2, α3 and α5 is significantly smaller for the *Hp*-SK enzyme and this proved to have an intrinsically different motion for the two enzymes.

Compounds **3**–**6** are reversible competitive inhibitors of both SK enzymes but, in general, they are more potent against the *H. pylori*, having K_i values in the low micromolar or nanomolar range. Compounds **3**, which contain an *O*-benzyl moiety, were the best inhibitors for both enzymes. Among the *O*-benzyl series **3**, the 3-nitrobenzyl derivative **3e** was found to be the most potent against the two enzymes and this compound had K_i values of 460 nM and 10 μM against *Hp*-SK and *Mt*-SK, respectively. The results of our MD simulation studies revealed that the 3-nitrobenzyl derivative **3e** would cause the opening of the LID domain (9 Å) and α-helix α3 (5 Å) of the SB domain of *Mt*-SK and a large conformational change in the position of the essential arginine by establishing a cation-π interaction with the nitrobenzyl ring of the ligand, with the nitro group pointing towards the SB domain. In contrast, for the *Hp*-SK enzyme, compound **3e** would mainly cause the opening of the region between α-helices α3 and α5 instead of α-helix α3, an interaction with the essential arginine would not be established and the nitro group would be oriented towards the LID domain.

5-Benzothiophenyl derivative **3i** proved to be a potent reversible competitive inhibitor of *Hp*-SK (K_i = 560 nM). This compound would stabilize an open conformation of the LID (5 Å) and SB (3 Å) domains through a set of favorable apolar interactions with this ‘dynamic apolar pocket’. Moreover, compound **10i**, a prodrug of inhibitor **3i**, was the most efficient derivative in achieving good *in vitro* activity against *Helicobacter pylori*, having a MIC value of 4 μg/mL.

The results from the studies described here have identified a good scaffold for the design of reversible competitive inhibitors of the SK enzyme and have opened up new opportunities for the development of novel inhibitors by targeting the dynamic apolar pocket that surrounds the C4 and C5 hydroxyl groups of the natural substrate. Moreover, these studies also represent a good example of the importance in drug design of taking into account the motion of an enzyme target. Thus,

stabilization of the inactive and inappropriate conformation for enzymatic catalysis seems to also be a good approach for the development of inhibitors that can be used as drugs.

Experimental Section

General. All starting materials and reagents were commercially available and were used without further purification unless is indicated. ^{1}H NMR spectra (250, 300 and 500 MHz), ^{13}C NMR spectra (63, 75 and 125 MHz), ^{31}P NMR spectra (202 MHz) and ^{19}F NMR spectra (282 MHz) were measured in deuterated solvents. *J* values are given in Hertz. NMR assignments were carried out by a combination of 1 D, COSY, and DEPT-135 experiments. FT-IR spectra were recorded as NaCl plates or KBr discs in a PerkinElmer Two FTIR spectrometer with attenuated total reference. $[\alpha]_D^{20}$ = values are given in 10^{-1} deg cm^2 g^{-1}. MilliQ deionized water was used in all the buffers. All procedures involving the use of ion-exchange resins were carried out at room temperature using Milli-Q deionized water. Amberlite IR-120 (H^+) (cation exchanger) was washed alternately with water, 10% NaOH, water, 10% HCl, and finally water before use. The spectroscopic measurements were made on a Varian Cary 100 UV-Vis spectrophotometer with a 1 cm pathlength cell fitted with a Peltier temperature controller. The purity of compounds **3**–**6** was analyzed by HPLC and by NMR. For compounds **3**–**5**, HPLC was performed on a Bio-Rad Aminex ion exclusion HPX-87H organic acids column (300 mm × 16 mm), eluting with 100 mM aqueous formic acid at a flow rate of 0.6 mL min^{-1}. For compounds **6**, a Phenomenex Luna 5 µM C18 column (250 mm × 4.6 mm), eluting with a gradient of acetonitrile/water [from (5:95) to (30:70)] at a flow rate of 1 mL min^{-1}, was employed. All tested compounds have a purity ≥95%.

General procedure for the synthesis of compounds 9 – A solution of alcohol **8**[22] (1 equivalent), *N*,*N*-diisopropylethylamine (1.6 equivalents), benzyl bromide (1.5 equivalents) and sodium iodide (0.1 equivalents) under inert atmosphere, was heated at 150 °C for 1.5–4.5 h. After cooling to room temperature, the resulting brown residue was dissolved in a mixture of ethyl acetate and saturated

solution of sodium bisulfate. The organic layer was separated and the aqueous layer was extracted with ethyl acetate (×3). The combined organic extracts were dried (Na_2SO_4 anh.), filtered and concentrated under reduced pressure. The resulted reside was purified by flash chromatography to give benzyl ethers **9**.

Methyl (3*R*,4*S*,5*R*)-5-benzyloxy-3,4-(*O*-isopropiliden)cyclohex-1-ene-1-carboxylate (9a) – Alcohol **8** (100 mg, 0.44 mmol), *N*,*N*-diisopropylethylamine (0.12 mL, 0.70 mmol), benzyl bromide (78 μL, 0.66 mmol) and sodium iodide (6.6 mg, 0.044 mmol). Reaction time = 4.5 h. Chromatographic eluent: (20:80) diethyl ether/hexane. **9a** (47 mg, 39%) as a yellow oil. $[\alpha]_D^{20}$= –39.0º (*c*2.0, $CHCl_3$). ^{1}H NMR (300 MHz, $CDCl_3$) δ: 7.30 (m, 5H, 5×ArH), 6.88 (m, 1H, H2), 4.75 (m, 1H, H3), 4.70 (d, *J* = 12.0 Hz, 1H, OC*H*H), 4.64 (d, *J* = 12.0 Hz, 1H, OC*H*H), 4.26 (t, *J* = 6.3 Hz, 1H, H4), 3.77 (m, 1H, H5), 3.76 (s, 3H, OCH_3), 2.70 (dd, *J* = 4.2 and 17.4 Hz, 1H, $H6_{eq}$), 2.40 (dd, *J* = 6.6 and 17.4 Hz, 1H, $H6_{ax}$) and 1.39 (br s, 6H, 2×CH_3) ppm. ^{13}C NMR (75 MHz, $CDCl_3$) δ: 166.7 (C), 138.1 (C), 134.6 (CH), 129.5 (C), 128.3 (2×CH), 127.6 (3×CH), 109.4 (C), 75.9 (CH), 74.6 (CH), 72.3 (CH), 71.5 (OCH_2), 52.0 (OCH_3), 27.8 (CH_3), 26.1 (CH_2) and 25.8 (CH_3) ppm. IR (film) υ: 1722 (CO) cm^{-1}. MS (ESI) *m/z* = 341 (MNa^+). HRMS calcd for $C_{18}H_{22}O_5Na$ (MNa^+): 341.1359, found 341.1352.

Methyl (3*R*,4*S*,5*R*)-5-(3-methoxybenzyloxy)-3,4-(*O*-isopropiliden)cyclohex-1-ene-1-carboxylate (9b) – Alcohol **8** (100 mg, 0.44 mmol), *N*,*N*-diisopropylethylamine (0.12 mL, 0.70 mmol), 3-metoxybenzyl bromide (92 μL, 0.66 mmol) and sodium iodide (6.6 mg, 0.044 mmol). Reaction time = 1.5 h. Chromatographic eluent: (25:75) diethyl ether/hexane. **9b** (47 mg, 31%) as a yellow oil. $[\alpha]_D^{20}$= –93.2º (*c*0.2, $CHCl_3$). ^{1}H NMR (300 MHz, $CDCl_3$) δ: 7.23 (t, *J* = 7.8 Hz, 1H, ArH), 6.92–6.80 (m, 4H, 3×ArH+H2), 4.74 (m, 1H, H3), 4.66 (d, *J* = 12.6 Hz, 1H, OC*H*H), 4.62 (d, *J* = 12.6 Hz, 1H, OC*H*H), 4.25 (t, *J* = 6.3 Hz, 1H, H4), 3.79 (s, 3H, OCH_3), 3.75 (s, 3H, OCH_3), 2.69 (dd, *J* = 3.6 and 17.4 Hz, 1H, $H6_{eq}$), 2.39 (dd, *J* = 6.6 and 17.4 Hz, 1H, $H6_{ax}$) and 1.38 (br s, 6H, 2×CH_3) ppm.

^{13}C NMR (75 MHz, $CDCl_3$) δ: 166.7 (C), 159.7 (C), 139.8 (C), 134.6 (CH), 129.5 (C), 129.3 (CH), 119.9 (CH), 113.2 (CH), 113.0 (CH), 109.4 (C), 75.9 (CH), 74.6 (CH), 72.3 (CH), 71.4 (OCH_2), 55.1 (OCH_3), 52.0 (OCH_3), 27.8 (CH_3), 26.1 (CH_2) and 25.8 (CH_3) ppm. IR (film) υ: 1710 (CO) cm^{-1}. MS (ESI) *m/z* = 371 (MNa^+). HRMS calcd for $C_{19}H_{24}O_6Na$ (MNa^+): 371.1465, found 371.1469.

Methyl (3*R*,4*S*,5*R*)-5-(3-fluorobenzyloxy)-3,4-(*O*-isopropiliden)cyclohex-1-ene-1-carboxylate (**9c**) **–** Alcohol **8** (100 mg, 0.44 mmol), *N*,*N*-diisopropylethylamine (0.12 mL, 0.70 mmol), 3-fluorobenzyl bromide (81 μL, 0.66 mmol) and sodium iodide (6.6 mg, 0.044 mmol). Reaction time = 2 h. Chromatographic eluent: (30:70) diethyl ether/hexane. **9c** (61 mg, 47%) as a yellow oil. $[\alpha]_D^{20} = -63.4^o$ (*c*0.8, $CHCl_3$). ^{1}H NMR (300 MHz, $CDCl_3$) δ: 7.27 (m, 1H, ArH), 7.08 (m, 2H, 2×ArH), 6.97–6.89 (m, 2H, ArH+H2), 4.75 (m, 1H, H3), 4.68 (d, *J* = 13.2 Hz, 1H, OC*H*H), 4.64 (d, *J* = 13.2 Hz, 1H, OC*H*H), 4.25 (t, *J* = 6.6 Hz, 1H, H4), 3.76 (s, 3H, OCH_3), 3.67 (m, 1H, H5), 2.72 (dd, *J* = 3.6 and 17.4 Hz, 1H, $H6_{eq}$), 2.36 (dd, *J* = 6.9 and 17.4 Hz, 1H, $H6_{ax}$) and 1.39 (s, 6H, 2×CH_3) ppm. ^{13}C NMR (75 MHz, $CDCl_3$) δ: 166.6 (C), 162.9 (C, J_{C-F} = 244 Hz), 140.9 (C, J_{C-F} = 7 Hz), 134.5 (CH), 129.8 (CH, J_{C-F} = 8 Hz), 129.6 (C), 122.8 (CH, J_{C-F} = 3 Hz), 114.5 (CH, J_{C-F} = 32 Hz), 114.2 (CH, J_{C-F} = 34 Hz), 109.5 (C), 76.1 (CH), 75.0 (CH), 72.3 (CH), 70.7 (OCH_2), 52.0 (OCH_3), 27.7 (CH_3), 26.2 (CH_2) and 25.7 (CH_3) ppm. IR (film) υ: 1710 (CO) cm^{-1}. MS (ESI) *m/z* = 359 (MNa^+). HRMS calcd for $C_{18}H_{21}O_5FNa$ (MNa^+): 359.1265, found 359.1269.

Methyl (3*R*,4*S*,5*R*)-5-(3-methylbenzyloxy)-3,4-(*O*-isopropiliden)cyclohex-1-ene-1-carboxylate (**9d**) **–** Alcohol **8** (284.5 mg, 2.25 mmol), *N*,*N*-diisopropylethylamine (0.35 mL, 2.0 mmol), 3-methylbenzyl bromide (0.25 mL, 1.88 mmol) and sodium iodide (19 mg, 0.125 mmol). Reaction time = 1.5 h. Chromatographic eluent: (40:60) diethyl ether/hexane. **9d** (166.3 mg, 40%) as a yellow oil. $[\alpha]_D^{20} = -55.7^o$ (*c*1.0, $CHCl_3$). ^{1}H NMR (250 MHz, $CDCl_3$) δ: 7.21 (d, *J* = 7.3 Hz, 1H, ArH), 7.16 (s, 2H, 2×ArH), 7.10 (t, *J* = 5.5 Hz, 1H, ArH), 6.89 (m, 1H, H2), 4.76 (m, 1H, H3), 4.67 (d, *J* = 12.0 Hz, 1H, OC*H*H), 4.61 (d, *J* = 12.0 Hz, 1H, OCH*H*), 4.26 (t, *J* = 6.3 Hz, 1H, H4), 3.79 (m, 1H, H5),

3.77 (s, 3H, OCH_3), 2.76–2.67 (m, 1H, $H6_{ax}$), 2.40–2.35 (m, 1H, $H6_{eq}$), 2.35 (s, 3H, CH_3) and 1.40 (s, 6H, 2×CH_3) ppm. ^{13}C NMR (63 MHz, $CDCl_3$) δ: 166.8 (C), 138.0 (2×C), 134.7 (CH), 129.6 (C), 128.5 (2×CH), 128.3 (CH), 124.9 (CH), 109.4 (C), 75.9 (CH), 74.5 (CH), 72.3 (OCH_3), 71.5 (OCH_2), 52.1 (CH), 27.9 (CH_3), 26.1 (CH_2), 25.9 (CH_3) and 21.4 (CH_3) ppm. IR (ATR) υ: 1714 (CO) cm^{-1}. MS (ESI) *m/z* = 355 (MNa^+). HRMS calcd for $C_{19}H_{24}NaO_5$ (MNa^+): 355.1516; found, 355.1516.

Methyl (3*R*,4*S*,5*R*)-5-(3-nitrobenzyloxy)-3,4-(*O*-isopropyliden)cyclohex-1-eno-1-carboxylate (9e) – Alcohol **8** (115 mg, 0.50 mmol), *N*,*N*-diisopropylethylamine (0.14 mL, 0.80 mmol), 3-nitrobenzyl bromide (162 mg, 0.75 mmol) and sodium iodide (7.5 mg, 0.05 mmol). Reaction time = 1.5 h. Chromatographic eluent: (30:70) ethyl acetate/hexane. **9e** (58.1 mg, 32%) as a yellow oil. $[\alpha]_D^{20}$ = –51.8º (*c*1.3, $CHCl_3$). ^{1}H NMR (300 MHz, $CDCl_3$) δ: 8.22 (br s, 1H, ArH), 8.13 (d, *J* = 8.4 Hz, 1H, ArH), 7.68 (d, *J* = 7.6 Hz, 1H, ArH), 7.50 (t, *J* = 8.0 Hz, 1H, ArH), 6.91 (br s, 1H, H2), 4.77 (s, 2H, OCH_2), 4.70 (br s, 1H, H3), 4.22 (t, *J* = 6.6 Hz, 1H, H4), 3.77 (s, 3H, OCH_3), 3.72 (m, 1H, H5), 2.78 (dd, *J* = 3.5 and 17.5 Hz, 1H, $H6_{ax}$), 2.40−2.32 (m, 1H, $H6_{eq}$) and 1.40 (s, 6H, 2×CH_3) ppm. ^{13}C NMR (63 MHz, $CDCl_3$) δ: 166.6 (C), 148.4 (C), 140.7 (C), 134.7 (CH), 133.4 (CH), 129.8 (C), 129.4 (CH), 122.7 (CH), 122.4 (CH), 109.7 (C), 76.5 (CH), 76.1 (CH), 72.5 (CH), 70.5 (OCH_2), 52.3 (OCH_3), 27.9 (CH_3), 26.6 (CH_2) and 25.8 (CH_3) ppm. IR (ATR) υ: 1710 (CO) and 1531 (NO) cm^{-1}. MS (ESI) *m/z* = 386 (MNa^+). HRMS calcd for $C_{18}H_{21}NO_7Na$ (MNa^+): 386.1210; found, 386.1216.

Methyl (3*R*,4*S*,5*R*)-5-(4-methylbenzyloxy)-3,4-(*O*-isopropiliden)cyclohex-1-ene-1-carboxylate (9f) – Alcohol **8** (250 mg, 1.10 mmol), *N*,*N*-diisopropylethylamine (0.30 mL, 1.76 mmol), 4-methylbenzyl bromide (305 mg, 1.65 mmol) and sodium iodide (16 mg, 0.11 mmol). Reaction time = 1.5 h. Chromatographic eluent: (40:60) diethyl ether/hexane. **9f** (307 mg, 84%) as a yellow oil. $[\alpha]_D^{20}$ = –50.2º (*c*1.1, $CHCl_3$). ^{1}H NMR (300 MHz, $CDCl_3$) δ: 7.23 (d, *J* = 8.0 Hz, 2H, 2×ArH), 7.13

(d, *J* = 8.2 Hz, 2H, 2×ArH), 6.87 (m, 1H, H2), 4.73 (m, 1H, H3), 4.65 (d, *J* = 12.0 Hz, 1H, OC*H*H), 4.59 (d, *J* = 12.0 Hz, 1H, OCH*H*), 4.24 (t, *J* = 6.2 Hz, 1H, H4), 3.77 (m, 1H, H5), 3.75 (s, 3H, OCH_3), 2.71–2.64 (m, 1H, $H6_{ax}$), 2.45–2.36 (m, 1H, $H6_{eq}$), 2.33 (s, 3H, CH_3) and 1.38 (s, 6H, 2×CH_3) ppm. ^{13}C NMR (75 MHz, $CDCl_3$) δ: 166.7 (C), 137.3 (C), 135.1 (C), 134.7 (CH), 129.5 (C), 129.0 (2×CH), 127.8 (2×CH), 109.3 (C), 75.8 (CH), 74.3 (CH), 72.3 (CH), 71.3 (OCH_2), 51.9 (OCH_3), 27.8 (CH_3), 26.1 (CH_2), 25.9 (CH_3) and 21.1 (CH_3) ppm. IR (ATR) υ: 1720 (CO) cm^{-1}. MS (ESI) *m/z* = 355 (MNa^+). HRMS calcd for $C_{19}H_{24}NaO_5$ (MNa^+): 355.1516; found, 355.1517.

Methyl (3*R*,4*S*,5*R*)-3,4-(*O*-isopropiliden)-5-(perfluorobenzyl)cyclohex-1-ene-1-carboxylate (9g) – Alcohol **8** (200 mg, 0.88 mmol), *N*,*N*-diisopropylethylamine (0.24 mL, 1.41 mmol), perfluorobenzyl bromide (0.2 mL, 1.32 mmol) and sodium iodide (13.2 mg, 0.09 mmol). Reaction time = 1.5 h. Chromatographic eluent: (10:90) diethyl ether/hexane. **9g** (40 mg, 11%) as a yellow oil. $[\alpha]_D^{20} = -27.0°$ (*c*0.6, $CHCl_3$). ^{1}H NMR (500 MHz, $CDCl_3$) δ: 6.89 (m, 1H, H2), 4.75 (dt, *J* = 2.0 and 8.5 Hz, 1H, OCH_2), 4.72 (m, 1H, H3), 4.19 (t, *J* = 6.5 Hz, 1H, H4), 3.77 (s, 3H, OCH_3), 3.73 (dt, *J* = 4.5 and 7.0 Hz, 1H, H5), 2.73 (ddt, *J* = 17.5, 4.5 and 1.5 Hz, 1H, $H6_{eq}$), 2.34 (ddt, *J* = 17.5, 2.9 and 7.5 Hz, 1H, $H6_{ax}$), 1.40 (s, 3H, CH_3) and 1.39 (s, 3H, CH_3) ppm. ^{13}C NMR (125 MHz, $CDCl_3$) δ: 166.5 (C), 146.6–136.4 (m, 5×C), 134.5 (CH), 129.5 (C), 111.4 (td, $J_{C\text{-}F}$ = 2 and 11 Hz, C), 109.6 (C), 76.4 (CH), 76.1 (CH), 72.3 (CH), 58.8 (OCH_2), 52.1 (OCH_3), 27.7 (CH_3), 26.4 (CH_2) and 25.7 (CH_3) ppm. ^{19}F NMR (282 MHz, $CDCl_3$) δ: −142.9 (dd, *J* = 5 and 20 Hz, 2F), −153.9 (t, *J* = 20 Hz, 1F) and −162.1 (dt, *J* = 7 and 20 Hz, 2F) ppm. IR (film) υ: 1722 (CO) cm^{-1}. MS (ESI) *m/z* = 431 (MNa^+). HRMS calcd for $C_{18}H_{17}F_5O_5Na$ (MNa^+): 431.0888; found, 431.0889.

Methyl (3*R*,4*S*,5*R*)-5-(2-naphthyl)methoxy-3,4-(*O*-isopropiliden)cyclohex-1-ene-1-carboxylate (9h) – Alcohol **8** (100 mg, 0.44 mmol), *N*,*N*-diisopropylethylamine (0.12 mL, 0.70 mmol), 2-(bromomethyl)naphatalene (150 mg, 0.66 mmol) and sodium iodide (6.6 mg, 0.044 mmol). Reaction time = 3 h. Chromatographic eluent: gradient of diethyl ether/hexanes [(15:85) to (20:80)]. **9h** (85

mg, 59%) as a yellow oil. $[\alpha]_D^{20} = -52.1^{o}$ (*c*0.9, $CHCl_3$). ^{1}H NMR (300 MHz, $CDCl_3$) δ: 7.81 (m, 4H, 4×ArH), 7.48 (m, 3H, 3×ArH), 6.91 (m, 1H, H2), 4.87 (d, *J* = 12.6 Hz, 1H, OC*H*H), 4.82 (d, *J* = 12.6 Hz, 1H, OC*H*H), 4.78 (m, 1H, H3), 4.31 (t, *J* = 6.3 Hz, 1H, H4), 3.84 (m, 1H, H5), 3.76 (s, 3H, OCH_3), 2.75 (dd, *J* = 4.2 and 17.4 Hz, 1H, $H6_{eq}$), 2.45 (dd, *J* = 6.6 and 17.4 Hz, 1H, $H6_{ax}$) and 1.41 (br s, 6H, 2×CH_3) ppm. ^{13}C NMR (75 MHz, $CDCl_3$) δ: 166.7 (C), 135.6 (C), 134.6 (CH), 133.2 (C), 133.0 (C), 129.5 (C), 128.1 (CH), 127.8 (CH), 127.6 (CH), 126.4 (CH), 126.0 (CH), 125.8 (CH), 125.6 (CH), 109.4 (C), 75.9 (CH), 74.6 (CH), 72.3 (CH), 71.6 (OCH_2), 52.0 (OCH_3), 27.8 (CH_3), 26.2 (CH_2) and 25.8 (CH_3) ppm. IR (film) υ: 1710 (CO) cm^{-1}. MS (ESI) *m/z* = 391 (MNa^+). HRMS calcd for $C_{22}H_{24}O_5Na$ (MNa^+): 391.1516; found, 391.1523.

Methyl (3*R*,4*S*,5*R*)-5-(benzo[*b*]thiophen-5-ylmethoxy)-3,4-(*O*-isopropiliden)cyclohex-1-ene-1-carboxylate (**9i**) – Alcohol **8** (250 mg, 1.1 mmol), *N*,*N*-diisopropylethylamine (0.3 mL, 1.8 mmol), 5-(bromomethyl)benzo[*b*]thiophene (373 mg, 1.6 mmol) and sodium iodide (16.5 mg, 0.11 mmol). Reaction time = 1.5 h. Chromatographic eluent: (40:60) diethyl ether/hexane. **9i** (137 mg, 33%) as a yellow oil. $[\alpha]_D^{20} = -42.2°$ (*c*1.6, $CHCl_3$). ^{1}H NMR (300 MHz, $CDCl_3$) δ: 7.84 (d, *J* = 8.4 Hz, 1H, ArH), 7.80 (s, 1H, ArH), 7.43 (d, *J* = 5.4 Hz, 1H, ArH), 7.32 (m, 2H, 2×ArH), 6.89 (m, 1H, H2), 4.81 (d, *J* = 12.0 Hz, 1H, OC*H*H), 4.76 (m, 2H, OCH*H*+H3), 4.28 (t, *J* = 6.3 Hz, 1H, H4), 3.81 (m, 1H, H5), 3.75 (s, 3H, OCH_3), 2.73 (dd, *J* = 4.5 and 17.4 Hz, 1H, $H6_{eq}$), 2.42 (dd, *J* = 6.6 and 17.4 Hz, 1H, $H6_{ax}$), 1.40 (s, 3H, CH_3) and 1.39 (s, 3H, CH_3) ppm. ^{13}C NMR (75 MHz, $CDCl_3$) δ: 166.6 (C), 139.6 (C), 139.0 (C), 134.5 (CH), 134.2 (C), 129.5 (C), 124.1 (CH), 123.7 (CH), 122.7 (CH), 122.5 (CH), 122.3 (CH), 109.3 (C), 75.9 (CH), 74.4 (CH), 72.2 (CH), 71.5 (CH_2), 51.9 (OCH_3), 27.7 (CH_3), 26.1 (CH_2) and 25.8 (CH_3) ppm. IR (ATR) υ: 1710 (CO) cm^{-1}. MS (ESI) *m/z* = 397 (MNa^+). HRMS calcd for $C_{20}H_{22}O_5SNa$(MNa^+): 397.1080; found, 397.1091.

General procedure for the synthesis of compounds 10 – A solution of acetal **9** (1 equivalent) in ethanol (0.15 M) and aqueous solution of HCl (0.16 mL/mmol, 6 M) was heated at 60 °C for 1.5–4

h. After cooling to room temperature, the reaction mixture was concentrated under reduced pressure and the resulting residue was purified by flash chromatography to give diol **10**.

Methyl (3*R*,4*S*,5*R*)-5-benzyloxy-3,4-dihydroxycyclohex-1-ene-1-carboxylate (**10a**) – Acetal **9a** (45.8 mg, 0.15 mmol), ethanol (1 mL) and HCl (25 μL, 6 M). Reaction time = 4 h. Chromatographic eluent: (75:25) diethyl ether/hexane. **10a** (40 mg, 95%) as a yellow oil. $[\alpha]_D^{20} = -133.9^{o}$ (*c*3.2, $CHCl_3$). ^{1}H NMR (300 MHz, $CDCl_3$) δ: 7.34 (m, 5H, 5×ArH), 6.86 (m, 1H, H2), 4.71 (d, *J* = 11.4 Hz, 1H, OC*H*H), 4.51 (d, *J* = 11.4 Hz, 1H, OC*H*H), 4.48 (t, *J* = 4.2 Hz, 1H, H3), 3.88–3.78 (m, 2H, H4+H5), 3.76 (s, 3H, OCH_3), 2.93 (dd, *J* = 4.2 and 17.7 Hz, 1H, $H6_{ax}$) and 2.27 (br dd, *J* = 6.9 and 17.7 Hz, 1H, $H6_{ax}$) ppm. ^{13}C NMR (75 MHz, $CDCl_3$) δ: 166.8 (C), 137.8 (C), 136.0 (CH), 130.2 (C), 128.5 (CH), 127.9 (CH), 127.6 (CH), 74.1 (CH), 71.4 (OCH_2), 70.9 (CH), 65.8 (CH), 52.0 (OCH_3) and 28.5 (CH_2) ppm. IR (film) υ: 3423 (OH) and 1715 (CO) cm^{-1}. MS (ESI) *m/z* = 301 (MNa^+). HRMS calcd for $C_{15}H_{18}O_5Na$ (MNa^+): 301.1046; found, 301.1039.

Methyl (3*R*,4*S*,5*R*)-3,4-dihydroxy-5-(3-methoxybenzyloxy)cyclohex-1-ene-1-carboxylate (**10b**) – Acetal **9b** (37 mg, 0.11 mmol), ethanol (0.7 mL) and HCl (18 μL, 6 M). Reaction time = 1.5 h. Chromatographic eluent: (80:20) ethyl acetate/hexane. **10b** (30 mg, 90%) as a colourless oil. $[\alpha]_D^{20} = -114.8^{o}$ (*c*2.9, $CHCl_3$). ^{1}H NMR (300 MHz, $CDCl_3$) δ: 7.26 (t, *J* = 7.8 Hz, 1H, ArH), 6.87 (m, 4H, 3×ArH+H2), 4.69 (d, *J* = 11.7 Hz, 1H, OC*H*H), 4.48 (m, 2H, OCH*H*+H3), 3.82 (m, 2H, H4+H5), 3.80 (s, 3H, OCH_3), 3.75 (s, 3H, OCH_3), 2.93 (dd, *J* = 3.9 and 18.3 Hz, 1H, $H6_{eq}$) and 2.26 (dd, *J* = 6.3 and 18.3 Hz, 1H, $H6_{ax}$) ppm. ^{13}C NMR (75 MHz, $CDCl_3$) δ: 166.7 (C), 159.7 (C), 139.4 (C), 135.9 (CH), 130.3 (C), 129.6 (CH), 120.0 (CH), 113.3 (CH), 74.1 (CH), 71.3 (OCH_2), 71.0 (CH), 65.8 (CH), 55.2 (OCH_3), 52.1 (OCH_3) and 28.6 (CH_2) ppm. IR (film) υ: 3432 (OH) and 1715 (CO) cm^{-1}. MS (ESI) *m/z* = 331 (MNa^+). HRMS calcd for $C_{16}H_{20}O_6Na$ (MNa^+): 331.1152; found, 331.1156.

Methyl (3*R*,4*S*,5*R*)-5-(3-fluorobenzyloxy)-3,4-dihydroxycyclohex-1-ene-1-carboxylate (**10c**) – Acetal **9c** (47 mg, 0.14 mmol), ethanol (0.9 mL) and HCl (25 μL, 6 M). Reaction time = 4 h. Chromatographic eluent: (70:30) ethyl acetate/hexane. **10c** (41 mg, 99%) as a yellow oil. $[\alpha]_D^{20} = -113.0^o$ (*c*4.2, $CHCl_3$). ^{1}H NMR (300 MHz, $CDCl_3$) δ: 7.30 (m, 1H, ArH), 7.09–6.95 (m, 3H, ArH), 6.90 (m, 1H, H2), 4.69 (d, *J* = 12.0 Hz, 1H, C*H*H), 4.52 (d, *J* = 12.0 Hz, 1H, CH*H*), 4.49 (t, *J* = 3.9 Hz, 1H, H3), 3.83 (m, 2H, H4+H5), 3.75 (s, 3H, OCH_3), 2.90 (m, 1H, $H6_{ax}$) and 2.27 (m, 1H, $H6_{eq}$) ppm. ^{13}C NMR (75 MHz, $CDCl_3$) δ: 166.7 (C), 162.9 (C, J_{C-F} = 245 Hz), 140.5 (C, J_{C-F} = 7 Hz), 136.1 (CH), 130.0 (CH, J_{C-F} = 9 Hz), 123.0 (CH, J_{C-F} = 3 Hz), 114.7 (CH, J_{C-F} = 22 Hz), 114.4 (CH, J_{C-F} = 22 Hz), 74.4 (CH), 70.9 (CH), 70.6 (OCH_2), 65.9 (CH), 52.1 (OCH_3) and 28.4 (CH_2) ppm. IR (film) υ: 3431 (OH) and 1716 (CO) cm^{-1}. MS (ESI) *m/z* = 319 (MNa^+). HRMS calcd for $C_{15}H_{17}O_5FNa$ (MNa^+): 319.0952; found, 319.0949.

Methyl (3*R*,4*S*,5*R*)-3,4-dihydroxy-5-(3-nitrobenciloxy)cyclohex-1-ene-carboxylate (**10e**) – Acetal **9e** (56.2 mg, 0.15 mmol), ethanol (1 mL) and HCl (30 μL, 6 M). Reaction time = 3 h. Chromatographic eluent: (60:40) ethyl acetate/hexane. **10e** (27.2 mg, 56%) as a yellow oil. $[\alpha]_D^{20} = -171.5^o$ (*c*1.0, $CHCl_3$). ^{1}H NMR (300 MHz, $CDCl_3$) δ: 8.20 (br s, 1H, ArH), 8.13 (d, *J* = 8.1 Hz, 1H, ArH), 7.65 (d, *J* = 7.5 Hz, 1H, ArH), 7.51 (t, *J* = 7.9 Hz, 1H, ArH), 6.86 (br s, 1H, H2), 4.79 (d, *J* = 12.2 Hz, 1H, OC*H*H), 4.65 (d, *J* = 12.2 Hz, 1H, OCH*H*), 4.51 (br s, 1H, H3), 3.88 (m, 2H, H5+H4), 2.95 (s, 1H, OH), 2.85 (m, 2H, OH+$H6_{ax}$) and 2.29 (m, 1H, $H6_{eq}$) ppm. ^{13}C NMR (75 MHz, $CDCl_3$) δ: 166.8 (C), 148.4 (C), 140.3 (C), 136.3 (CH), 133.4 (CH), 130.1 (C), 129.6 (CH), 122.9 (CH), 122.3 (CH), 75.1 (CH), 71.0 (CH), 70.3 (CH), 66.1 (OCH_2), 52.3 (OCH_3) and 28.5 (CH_2) ppm. IR (ATR): 3415 (OH), 1710 (CO) and 1525 (NO) cm^{-1}. MS (ESI) *m/z* = 346 (MNa^+). HRMS calcd for $C_{15}H_{17}NO_7Na$ (MNa^+): 346.0897; found, 346.0907.

Methyl (3*R*,4*R*,5*R*)-3,4-dihydroxy-5-((perfluorophenyl)methoxy)cyclohex-1-ene-1-carboxylate (**10g**) – Acetal **9g** (73.5 mg, 0.18 mmol), ethanol (1.2 mL) and HCl (32 μL, 6 M). Reaction time = 2

h. Chromatographic eluent: (25:75) diethyl ether/hexane. **10g** (43.7 mg, 66%) as a colourless oil. $[\alpha]_D^{20} = -92.6°$ (*c*1.3, $CHCl_3$). ^{1}H NMR (500 MHz, $CDCl_3$) δ: 6.86 (m, 1H, H2), 4.79 (d, *J* = 11.0 Hz, 1H, OC*H*H), 4.65 (d, *J* = 11.0 Hz, 1H, OC*H*H), 4.46 (t, *J* = 4.0 Hz, 1H, H3), 3.84 (dt, *J* = 5.0 and 8.0 Hz, 1H, H5), 3.77–3.74 (m, 4H, OCH_3+H4), 2.97 (dd, *J* = 5.0 and 18.0 Hz, 1H, $H6_{ax}$) 2.75 (br s, 2H, 2×OH) and 2.28–2.23 (m, 1H, $H6_{eq}$) ppm. ^{13}C NMR (125 MHz, $CDCl_3$) δ: 166.6 (C), 146.6–136.5 (m, 5×C), 135.8 (CH), 130.0 (C), 111.0 (td, J_{C-F} = 3 and 18 Hz, C), 75.1 (CH), 70.9 (CH), 65.8 (CH), 58.4 (OCH_2), 52.1 (OCH_3) and 28.5 (CH_2) ppm. ^{19}F NMR (282 MHz, $CDCl_3$) δ: –143.1 (dd, *J* = 7 and 21 Hz, 2F), –153.2 (t, *J* = 21 Hz, 1F) and –161.5 (dt, *J* = 8 and 21 Hz, 2F) ppm. IR (film): 3332 (OH) and 1716 (CO) cm^{-1}. MS (ESI) *m/z* = 391 (MNa^+). HRMS calcd for $C_{15}H_{13}F_5O_5Na$ (MNa^+): 391.0575; found, 391.0575.

Methyl (3*R*,4*S*,5*R*)-3,4-dihydroxy-5-(2-naphthyl)methoxycyclohex-1-ene-1-carboxylate (**10h**) – Acetal **9h** (65 mg, 0.18 mmol), ethanol (1.2 mL) and HCl (30 μL, 6 M). Reaction time = 3 h. Chromatographic eluent: (60:40) ethyl acetate/hexane. **10h** (56 mg, 95%) as a colourless oil. $[\alpha]_D^{20} = -93.5°$ (*c*5.2, $CHCl_3$). ^{1}H NMR (300 MHz, $CDCl_3$) δ: 7.80 (m, 4H, 4×ArH), 7.47 (m, 3H, 3×ArH), 6.86 (t, *J* = 1.5 Hz, 1H, H2), 4.84 (d, *J* = 11.7 Hz, 1H, OC*H*H), 4.65 (d, *J* = 11.7 Hz, 1H, OC*H*H), 4.48 (m, 1H, H3), 3.85 (m, 2H, H4+H5), 3.75 (s, 3H, OCH_3), 3.00–2.90 (m, 3H, 2×OH+C*H*H), and 2.31 (dd, *J* = 6.3 and 17.7 Hz, 1H, CH*H*) ppm. ^{13}C NMR (75 MHz, $CDCl_3$) δ: 166.8 (C), 136.1 (CH), 135.2 (C), 133.2 (C), 133.0 (C), 130.1 (C), 128.3 (CH), 127.8 (CH), 127.6 (CH), 126.5 (CH), 126.3 (CH), 126.2 (CH), 126.0 (CH), 125.6 (CH), 74.1 (CH), 71.5 (OCH_2), 70.9 (CH), 65.9 (CH), 52.0 (OCH_3) and 28.5 (CH_2) ppm. IR (film) υ: 3427 (OH) and 1710 (CO) cm^{-1}. MS (ESI) *m/z* = 351 (MNa^+). HRMS calcd for $C_{19}H_{20}O_5Na$ (MNa^+): 351.1203; found, 351.1196.

Methyl (3*R*,4*S*,5*R*)-5-(benzo[*b*]thiophen-5-ylmethoxy)-3,4-dihydroxy-cyclohex-1-ene-1-carboxylate (**10f**) – Acetal **9f** (119.7 mg, 0.32 mmol), ethanol (2.1 mL) and HCl (57 μL, 6 M).

Reaction time = 4 h. Chromatographic eluent: (75:25) diethyl ether/hexane. **10h** (30.4 mg, 90%) as a colourless oil. $[\alpha]_D^{20} = -23.2°$ (*c*1.3, $CHCl_3$). ^{1}H NMR (300 MHz, $CDCl_3$) δ: 7.84 (d, *J* = 8.1 Hz, 1H, ArH), 7.76 (s, 1H, ArH), 7.44 (d, *J* = 5.4 Hz, 1H, ArH), 7.30 (m, 2H, 2×ArH), 6.84 (m, 1H, H2), 4.78 (d, *J* = 11.4 Hz, 1H, OC*H*H), 4.55 (d, *J* = 11.4 Hz, 1H, OCH*H*), 4.47 (m, 1H, H3), 3.89–3.76 (m, 2H, H4+H5), 3.74 (s, 3H, OCH_3), 3.10 (br s, 2H, 2×OH), 2.91 (dd, *J* = 4.2 and 17.7 Hz, 1H, $H6_{eq}$) and 2.30 (dd, *J* = 6.6 and 17.7 Hz, 1H, $H6_{ax}$) ppm. ^{13}C NMR (75 MHz, $CDCl_3$) δ: 166.8 (C), 139.6 (C), 139.2 (C), 136.2(CH), 133.9 (C), 130.0 (C), 127.0 (CH), 124.2 (CH), 123.7 (CH), 122.8 (CH), 122.5 (CH), 74.0 (CH), 71.4 (CH_2), 70.8 (CH), 65.9 (CH), 52.0 (OCH_3) and 28.4 (CH_2) ppm. IR (ATR) υ: 3406 (OH) and 1707 (CO) cm^{-1}. MS (ESI): 357 (MNa^+). HRMS calcd for $C_{17}H_{18}O_5SNa$ (MNa^+): 357.0767; found, 357.0772.

(3*R*,4*R*,5*R*)-3,4-dihydroxy-5-(3-methylbenzyloxy)cyclohex-1-ene-1-carboxylic acid (**3d**) – A solution of compound **9d** (166.3 mg, 0.50 mmol) in ethanol (3.4 mL) and aqueous solution of HCl (3.2 mL, 6 M) was heated at 60 °C for 3 h. After cooling to room temperature, the reaction mixture was concentrated under reduced pressure and the resulting residue was purified by flash chromatography, eluting with (60:40) ethyl acetate/hexane, to give acid **3d** (42.3 mg, 30%), as a yellow oil. $[\alpha]_D^{20} = -90.6°$ (*c*1.0, CH_3OH). ^{1}H NMR (300 MHz, CD_3OD) δ: 7.17–7.07 (m, 3H, 3×ArH), 7.02 (t, *J* = 7.0 Hz, 1H, ArH), 6.73 (br s, 1H, H2), 4.55 (d, *J* = 11.9 Hz, 1H, OC*H*H), 4.50 (d, *J* = 11.9 Hz, 1H, OCH*H*), 4.35 (br s, 1H, H3), 3.79 (m, 2H, H4+H5), 2.58 (br d, *J* = 18.3 Hz, 1H, $H6_{ax}$), 2.29 (m, 1H, $H6_{eq}$) and 2.26 (s, 3H, CH_3) ppm. ^{13}C NMR (75 MHz, CD_3OD) δ: 170.0 (C), 139.8 (C), 139.3 (CH), 139.0 (C), 130.3 (C), 129.4 (CH), 129.3 (CH), 129.2 (CH), 125.9 (CH), 76.4 (CH), 72.5 (OCH_2), 70.8 (CH), 67.4 (CH), 28.4 (CH_3) and 21.4 (CH_2) ppm. IR (ATR): 3409 (OH) and 1695 (CO) cm^{-1}. MS (ESI) *m/z* = 277 (M–H). HRMS calcd for $C_{15}H_{17}O_5$ (M–H): 277.1081; found, 277.1081.

(3*R*,4*R*,5*R*)-3,4-dihydroxy-5-(4-methylbenzyloxy)cyclohex-1-ene-1-carboxylic acid (**3f**) – A solution of compound **9f** (306.7 mg, 0.92 mmol) in ethanol (6.1 mL) and aqueous solution of HCl (6 mL, 6 M) was heated at 60 °C for 3 h. After cooling to room temperature, the reaction mixture was concentrated under reduced pressure and the resulting residue was purified by flash chromatography, eluting with (60:40) ethyl acetate/hexane, to give acid **3f** (84.3 mg, 33%), as a white solid. $[\alpha]_D^{20}$ = –78.0 º (*c*1.0, CH_3OH). Mp: 134.0–134.5 ˚C. ^{1}H NMR (300 MHz, CD_3OD) δ: 7.09 (d, *J* = 8.0 Hz, 2H, 2×ArH), 7.00 (d, *J* = 8.0 Hz, 2H, 2×ArH), 6.67 (m, 1H, H2), 4.47 (d, *J* = 11.8 Hz, 1H, OC*H*H), 4.42 (d, *J* = 11.8 Hz, 1H, OCH*H*), 4.26 (m, 1H, H3), 3.72 (m, 2H, H4+H5), 2.56–2.48 (m, 1H, $H6_{ax}$), 2.23–2.17 (m, 1H, $H6_{eq}$) and 2.17 (s, 3H, CH_3) ppm. ^{13}C NMR (75 MHz, CD_3OD) δ: 170.0 (C), 139.2 (CH), 138.4 (C), 136.8 (C), 130.3 (C), 129.9 (2×CH), 128.9 (2×CH), 76.2 (CH), 72.4 (OCH_2), 70.8 (CH), 67.5 (CH), 28.4 (CH_3) and 21.2 (CH_2) ppm. IR (ATR) υ: 3460 (OH), 3371 (OH) and 1688 (CO) cm^{-1}. MS (ESI) *m/z* = 277 (M–H). HRMS calcd for $C_{15}H_{17}O_5$ (M–H): 277.1081; found, 277.1081.

General procedure for the synthesis of compounds 3 – A solution of ester **10** (1 equivalent) in THF (0.1 M) was treated with an aqueous solution of lithium hydroxide (2.5 equivalents, 0.5 M). The resulting mixture was stirred at room temperature for 30 min and then MilliQ water was added. The organic solvent was removed under reduced pressure and the resulting aqueous solution was washed with diethyl ether (×3). The aqueous layer was treated with Amberlite IR-120 (H^+) until pH 6. The filtrate and the washings were lyophilized to give the acids **3**.

(3*R*,4*R*,5*R*)-5-benzyloxy-3,4-dihydroxycyclohex-1-ene-1-carboxylic acid (**3a**) – Ester **10a** (34 mg, 0.12 mmol), THF (1.2 mL) and LiOH (0.6 mL, 0.5 M). **3a** (24 mg, 76%) as a white solid. $[\alpha]_D^{20}$ = –92.0° (*c*2.6, MeOH). Mp: 210.7–212.2 ºC. ^{1}H NMR (300 MHz, CD_3OD) δ: 7.24 (m, 5H, 5×ArH), 6.60 (m, 1H, H2), 4.61 (d, *J* = 12 Hz, 1H, OC*H*H), 4.55 (d, *J* = 12 Hz, 1H, OCH*H*), 4.30 (m, 1H, H3), 3.77 (m, 2H, H4+H5), 2.68 (dd, *J* = 3.9 and 18 Hz, 1H, $H6_{ax}$) and 2.26 (dd, *J* = 2.2 and 19.7 Hz,

1H, $H6_{eq}$) ppm. ^{13}C NMR (75 MHz, CD_3OD) δ: 172.6 (C), 140.1 (C), 135.9 (CH), 133.6 (C), 129.3 (2×CH), 128.9 (2×CH), 128.6 (CH), 76.5 (CH), 72.5 (OCH_2), 71.8 (CH), 67.9 (CH) and 29.8 (CH_2) ppm. IR (ATR) υ: 3382 (OH), 3299 (OH) and 1686 (CO) cm^{-1}. MS (ESI): 263 (M–H). HRMS calcd for $C_{14}H_{15}O_5$ (M–H): 263.0925; found, 263.0918.

(3*R*,4*R*,5*R*)-3,4-dihydroxy-5-(3-methoxybenzyloxy)cyclohex-1-ene-1-carboxylic acid (**3b**) – Ester **10a** (27.6 mg, 0.09 mmol), THF (0.9 mL) and LiOH (0.46 mL, 0.5 M). **3b** (20.7 mg, 78%), as a white solid. $[\alpha]_D^{20} = -83.3°$ (*c*1.8, MeOH). Mp: 130.3–132.1 ºC. ^1H NMR (300 MHz, CD_3OD) δ: 7.19 (t, *J* = 7.5 Hz, 1H, ArH), 6.89 (m, 2H, 2×ArH), 6.78 (dd, *J* = 3.9 and 7.8 Hz, 1H, ArH), 6.63 (m, 1H, H2), 4.62 (d, *J* = 12.3 Hz, 1H, OC*H*H), 4.56 (d, *J* = 12.0 Hz, 1H, OCH*H*), 4.33 (m, 1H, H3), 3.79 (m, 2H, H4+H5), 3.75 (s, 3H, OCH_3), 2.70 (d, *J* = 17.7 Hz, 1H, $H6_{ax}$) and 2.28 (dd, *J* = 3.9 and 17.7 Hz, 1H, $H6_{eq}$) ppm. ^{13}C RMN (75 MHz, CD_3OD) δ: 174.9 (C), 163.8 (C), 144.2 (2×C), 138.6 (CH), 132.8 (CH), 123.5 (CH), 116.7 (CH), 116.6 (CH), 79.0 (CH), 74.9 (OCH_2), 74.2 (CH), 70.3 (CH), 58.1 (OCH_3) and 32.2 (CH_2) ppm. IR (ATR) υ: 3375 (OH) and 1686 (CO) cm^{-1}. MS (ESI): 293 (M–H). HRMS calcd for $C_{15}H_{17}O_6$ (M–H): 293.1031; found, 293.1027.

(3*R*,4*R*,5*R*)-5-(3-fluorobenzyloxy)-3,4-dihydroxycyclohex-1-ene-1-carboxylic acid (**3c**) – Ester **10c** (38.1 mg, 0.13 mmol), THF (1.3 mL) and LiOH (0.66 mL, 0.5 M). **3c** (24.8 mg, 68%), as a white solid. $[\alpha]_D^{20} = -78.4°$ (*c*2.9, MeOH). Mp: 123.9–124.4 ºC. ^1H NMR (300 MHz, CD_3OD) δ: 7.26 (dt, *J* = 6.9 and 9.0 Hz, 1H, 1×ArH), 7.07 (m, 2H, 2×ArH), 6.91 (dt, *J* = 2.7 and 10.5 Hz, 1H, 1×ArH), 6.66 (br s, 1H, H2), 4.62 (d, *J* = 15.0 Hz, 1H, OC*H*H), 4.56 (d, *J* = 15.0 Hz, 1H, OCH*H*), 4.31 (m, 1H, H3), 3.78 (m, 2H, H4+H5), 2.66 (m, 1H, $H6_{ax}$) and 2.25 (m, 1H, $H6_{eq}$) ppm. ^{13}C NMR (75 MHz, CD_3OD) δ: 171.4 (C), 164.4 (C, *J* = 291 Hz), 143.9 (C, *J* = 9 Hz), 137.4 (CH), 132.1 (C), 131.1 (CH, *J* = 10 Hz), 124.2 (CH, *J* = 3 Hz), 115.3 (CH, *J* = 3 Hz), 115.0 (CH, *J* = 1 Hz), 76.8 (CH), 71.7 (CH_2),

71.5 (CH), 67.7 (CH) and 29.3 (CH_2) ppm. IR (ATR) υ: 3407 (OH), 3312 (OH) and 1686 (CO) cm^{-1}. MS (ESI): 281 (M–H). HRMS calcd for $C_{14}H_{14}FO_5$ (M–H): 281.0831; found, 281.0823.

Sodium (3*R*,4*R*,5*R*)-3,4-dihydroxy-5-((3-nitrobenzyloxy)cyclohex-1-ene-1-carboxylate (**3e**) – A solution of ester **10e** (30 mg, 0.09 mmol) in THF (0.9 mL) was treated with an aqueous solution of sodium hydroxide (0.19 mL, 0.5 M). The resulting mixture was stirred at room temperature for 30 min and then MilliQ water was added. The organic solvent was removed under reduced pressure and the resulting aqueous solution was washed with diethyl ether (×2) and lyophilized to give the sodium salt **3e** (28 mg, 98%), as a brown foam. $[\alpha]_D^{20} = -23.7^o$ (*c*1.0, H_2O). ^{1}H NMR (300 MHz, D_2O) δ: 8.26 (br s, 1H, ArH), 8.18 (d, *J* = 7.6 Hz, 1H, ArH), 7.80 (d, *J* = 7.5 Hz, 1H, ArH), 7.60 (t, *J* = 7.9 Hz, 1H, ArH), 6.43 (br s, 1H, H2), 4.81 (d, *J* = 10.3 Hz, 1H, OC*H*H), 4.73 (d, *J* = 10.3 Hz, 1H, OCH*H*), 4.42 (br s, 1H, H3), 3.91 (m, 2H, H5+H4), 2.83 (dd, *J* = 4.1 and 17.5 Hz, 1H, $H6_{ax}$) and 2.26 (dd, *J* = 5.3 and 17.5 Hz, 1H, $H6_{eq}$) ppm. ^{13}C NMR (125 MHz, D_2O) δ: 175.1 (C), 147.8 (C), 139.7 (C), 135.4 (C), 134.7 (CH), 130.8 (CH), 129.7 (CH), 123.0 (CH), 122.8 (CH), 75.4 (CH), 70.4 (CH), 70.3 (OCH_2), 66.3 (CH) and 30.0 (CH_2) ppm. IR (ATR) υ: 3345 (OH), 1570 (CO) and 1531 (NO) cm^{-1}. MS (ESI) *m/z* = 332 (MNa^+). HRMS calcd for $C_{14}H_{15}NO_7Na$ (MNa^+): 332.0741; found, 332.0741.

Sodium (3*R*,4*R*,5*R*)-3,4-dihydroxy-5-((perfluorophenyl)methoxy)cyclohex-1-ene-1-carboxylate (**3g**) – A solution of ester **10g** (38.0 mg, 0.10 mmol) in THF (1.0 mL) was treated with an aqueous solution of sodium hydroxide (0.2 mL, 0.10 mmol, 0.5 M). The resulting mixture was stirred at room temperature for 6 h and then MilliQ water was added. The organic solvent was removed under reduced pressure and the resulting aqueous solution was washed with diethyl ether (×3) and lyophilized to give the sodium salt **3e** (38.5 mg, 99%), as a white solid. $[\alpha]_D^{20} = -71.4^o$ (*c*1.0, H_2O). Mp: 225.2 ºC (dec.). ^{1}H NMR (500 MHz, D_2O) δ: 6.43 (br s, 1H, H2), 4.88 (d, *J* = 12.0 Hz, 1H, OC*H*H), 4.86 (d, *J* = 12.0 Hz, 1H, OCH*H*), 4.39 (m, 1H, H3), 3.92 (m, 1H, H5), 3.84 (m, 1H, H4),

2.64 (dd, *J* = 4.0 and 18.0 Hz, 1H, $H6_{eq}$) and 2.23 (dd, *J* = 6.5 and 18.0 Hz, 1H, $H6_{ax}$) ppm. ^{13}C NMR (125 MHz, D_2O) δ: 175.0 (C), 146.4–136.3 (m, 5×C), 135.4 (C), 130.6 (CH), 110.6 (t, J_{C-F}= 10 Hz, C), 75.7 (CH), 70.2 (CH), 66.2 (CH), 58.5 (OCH_2) and 30.0 (CH_2) ppm. ^{19}F NMR (282 MHz, D_2O) δ: –143.8 (d, *J* = 16 Hz, 2F), –154.3 (t, *J* = 21 Hz, 1F) and –162.8 (dt, *J* = 6 and 21 Hz, 2F) ppm. IR (ATR) υ: 3371 (OH) and 1504 (CO) cm^{-1}. IR (ATR) υ: 3371 (OH) and 1504 (CO) cm^{-1}. MS (ESI) *m/z* = 353 (M–Na). HRMS calcd for $C_{14}H_{10}F_5O_5$ (M–Na): 353.0454; found, 353.0452.

(3*R*,4*R*,5*R*)-3,4-dihydroxy-5-(naphthy-2-yl)methoxycyclohex-1-ene-1-carboxylic acid (**3h**) – Ester **10h** (47 mg, 0.14 mmol), THF (1.4 mL) and LiOH (0.70 mL, 0.5 M). **3h** (19.6 mg, 45%), as a white solid. $[\alpha]_D^{20}$= –58.6° (*c*2.5, MeOH). Mp: 185.6–187.1 ºC. ^{1}H NMR (300 MHz, CD_3OD) δ: 7.82 (m, 4H, 4×ArH), 7.47 (m, 3H, 3×ArH), 6.74 (br s, 1H, H2), 4.83 (d, *J* = 12.0 Hz, 1H, OC*H*H), 4.77 (d, *J* = 12.0 Hz, 1H, OCH*H*), 4.41 (m, 1H, H3), 3.90 (m, 2H, H4+H5), 2.73 (br d, *J* = 18.3 Hz, 1H, $H6_{ax}$) and 2.37 (dd, *J* = 4.5 and 18.3 Hz, 1H, $H6_{eq}$) ppm. ^{13}C NMR (75 MHz, CD_3OD) δ: 171.3 (C), 137.8 (CH), 137.6 (C), 134.8 (C), 134.5 (C), 131.9 (C), 129.1 (CH), 128.9 (CH), 128.7 (CH), 127.5 (CH), 127.1 (CH), 127.0 (CH), 126.9 (2×CH), 76.6 (CH), 72.7 (CH_2), 71.4 (CH), 67.7 (CH) and 29.2 (CH_2) ppm. IR (ATR) υ: 3299 (OH) and 1686 (CO) cm^{-1}. MS (ESI): 313 (M–H). HRMS calcd for $C_{18}H_{17}O_5$ (M–H): 313.1081; found, 313.1092.

(3*R*,4*R*,5*R*)-5-(benzo[*b*]thiophen-5-yl)methoxy-3,4-dihydroxycyclohex-1-ene-1-carboxylic acid (**3i**) – Ester **10i** (83.5 mg, 0.25 mmol), THF (2.5 mL) and LiOH (1.25 mL, 0.5 M). **3i** (43.3 mg, 54%), as a white solid. Mp: 188.1–188.8 ºC. $[\alpha]_D^{20}$= –77.7° (*c*0.6, MeOH). ^{1}H NMR (300 MHz, CD_3OD) δ: 7.80 (m, 2H, 2×ArH), 7.50 (d, *J* = 5.1 Hz, 1H, ArH), 7.30 (d, *J* = 6.3 Hz, 2H, 2×ArH), 6.76 (br s, 1H, H2), 4.73 (d, *J* = 12.0 Hz, 1H, OC*H*H), 4.68 (d, *J* = 12.0 Hz, 1H, OCH*H*), 4.37 (br s, 1H, H3), 3.85 (br s, 2H, H4+H5), 2.64 (d, *J* = 18.0 Hz, 1H, C*H*H-6) and 2.32 (d, *J* = 18.0 Hz, 1H, CH*H*-6) ppm. ^{13}C NMR (75 MHz, CD_3OD) δ: 170.1 (C), 141.3 (C), 140.5 (C), 139.3 (CH), 136.2

(C), 130.4 (C), 127.9 (CH), 125.5 (CH), 124.9 (CH), 123.9 (CH), 123.3 (CH), 76.4 (CH), 72.6 (CH_2), 71.0 (CH), 67.6 (CH) and 28.6 (CH_2) ppm. IR (ATR) υ: 3396 (OH) and 1697 (CO) cm^{-1}. MS (ESI): 319 (M–H). HRMS calcd for $C_{16}H_{15}O_5S$ (M–H): 319.0646; found, 319.0644.

Methyl (3*S*,4*R*,5*R*)-3,4-dihydroxy-5-(mesyloxy)cyclohex-1-ene-1-carboxylate (12) – A solution of acetal **11**[24] (171 mg, 0.50 mmol) in dry dichloromethane (1.7 mL), under argon and at 0 ºC, was treated sucesively with dry trimethylamine (0.10 mL, 0.75 mmol) and mesyl chloride (50 µL, 0.60 mmol) dropwise. The resulting solution was stirred at room temperature for 1 h. The reaction mixture was treated with aqueous solution of potassium carbonate (20%) and then diluted with dichloromethane. The organic layer was separated and the aqueous layer was extracted with dichloromethane (×2). The combined organic extracts were dried (anh. Na_2SO_4), filtered and concentrated under reduced pressure. The resulting residue was dissolved in a mixture of methanol/water/HCl (c) (7.9 mL, 100:1:0.1) was stirred at room temperature for 15 min. The reaction mixture was neutralized with saturated solution of sodium bicarbonate followed by powdered sodium bicarbonate and then diluted with ethyl acetate. The organic layer was separated and the aqueous layer was extracted with ethyl acetate (×2). The combined organic extracts were washed with water (×3), brine (×2) and dried (anh. Na_2SO_4). The resulted organic extract was concentrated under reduced pressure and purified by flash chromatography, eluting with (60:40) ethyl acetate/hexane to give mesylate **12** (229 mg, 87%), as a white solid. $[\alpha]_D^{20} = -39.5^{o}$ (*c*1.2, CH_3OH). Mp: 144.0–144.4 ºC. ^{1}H NMR (250 MHz, CD_3OD) δ: 6.82 (m, 1H, H2), 4.85 (m, 1H, H5), 4.36 (m, 1H, H3), 3.89–3.83 (m, 1H, H4), 3.74 (s, 3H, OCH_3), 3.13 (s, 3H, CH_3), 2.99–2.89 (m, 1H, $H6_{ax}$) and 2.53–2.41 (m, 1H, $H6_{eq}$) ppm. ^{13}C NMR (63 MHz, CD_3OD) δ: 167.9 (C), 138.8 (CH), 129.4 (C), 79.2 (CH), 70.3 (CH), 67.0 (CH), 52.6 (OCH_3), 38.3 (CH_3) and 30.1 (CH_2) ppm. IR (ATR) υ: 3395 and 3301 (OH) and 1711 (CO) cm^{-1}. MS (ESI) *m/z* = 289 (MNa^+). HRMS calcd for $C_9H_{14}O_7SNa$ (MNa^+): 289.0352; found, 289.0350.

Epoxide 13. A solution of mesylate **12** (96 mg, 0.36 mmol) in dry methanol (0.5 mL) was treated with a solution of sodium methoxide (68 mg, 1.26 mmol) in dry methanol (0.55 mL). The resulting suspension was stirred at room temperature for 7 h. The solvent was concentrated under reduced pressure and the crude residue was dissolved in a mixture of dichloromethane and water. The organic layer was separated and the aqueous layer was extracted with dichloromethane (×2). The combined organic extracts were dried (anh. Na_2SO_4), filtered and concentrated under reduced pressure. The resulting residue was purified by flash chromatography, eluting with (40:60) ethyl acetate/hexane, to give epoxide **13**[25] (52 mg, 85%), as a colorless oil.

Methyl (3*R*,4*S*,5*R*)-5-azido-3,4-dihydroxycyclohex-1-ene-1-carboxylate (**14**). A solution of the epoxide **13** (21.5 mg, 0.13 mmol) in acetic acid (0.12 mL) was treated with sodium azide (44.2 mg, 0.68 mmol) in water (40 µL) and then heated at 40 ºC for 24 h. After cooling to room temperature, the reaction mixture was diluted with diethyl ether and water. The organic layer was separated and the aqueous layer was extracted with diethyl ether (×2). The combined organic extracts were washed with saturated $NaHCO_3$, dried (anh. Na_2SO_4), filtered and concentrated under reduced pressure. The resulting residue was purified by flash chromatography, eluting with (60:40) ethyl acetate/hexane, to give the azide **14**[23] (23.5 mg, 85%), as a white solid. Mp: 102.8–103.0 ˚C. $[\alpha]_D^{20}$= –167.0º (*c*1.1, $CHCl_3$). ^{1}H NMR (250 MHz, $CDCl_3$) δ: 6.88 (m, 1H, H2), 4.44 (t, *J* = 4.2 Hz, 1H, H3), 3.86 (m, 1H, H5), 3.77 (s, 3H, OCH_3), 3.70 (dd, *J* = 4.3 and 9.3 Hz, 1H, H4), 2.92 (dd, *J* = 5.4 and 17.9 Hz, 1H, $H6_{ax}$) and 2.33–2.21 (m, 1H, $H6_{eq}$) ppm. ^{13}C NMR (63 MHz, $CDCl_3$) δ: 166.3 (C), 135.8 (CH), 130.3 (C), 71.2 (CH), 65.5 (CH), 58.2 (OCH_3), 52.3 (CH) and 28.9 (CH_2) ppm. IR (ATR) υ: 3295 (OH), 2095 (N_3) and 1707 (CO) cm^{-1}.

Methyl (3*R*,4*S*,5*R*)-5-(4-benzyl-1*H*-1,2,3-triazol-1-yl)-3,4-dihydroxycyclohex-1-ene-1-carboxylate (15) – To a suspension of azide **14** (100 mg, 0.47 mmol) and 3-phenyl-1-propine (0.06 mL, 0.47 mmol) in a 1:1 mixture of *t*-BuOH-water (1.5 mL) freshly prepared aqueous sodium

ascorbate solution (0.47 mL, 1.0 M), followed by aqueous copper(II) sulphate solution (1.5 mL, 0.32 M) were added. The resultant heterogenous mixture was stirred vigorously during 16 h and then diluted with water and ethyl acetate. The organic layer was separated and the aqueous phase was extracted with ethyl acetate (×2). All the combined organic extracts were dried (anh. Na_2SO_4), filtered and evaporated. The obtained residue was purified by flash chromatography, eluting with (50:50) ethyl acetate/hexane, to afford triazol **15** (99.4 mg, 64%), as a white solid. $[\alpha]_D^{20} = -87.1^o$ (*c*1.1, MeOH). Mp: 153.8−154.5 ˚C. ^{1}H NMR (300 MHz, CD_3OD) δ: 7.77 (br s, 1H, ArH), 7.27 (m, 4H, 4×ArH), 7.21 (m, 1H, ArH), 6.96 (br d, *J* = 3.0 Hz, 1H, H2), 4.81 (m, 1H, H5), 4.34 (t, *J* = 4.1 Hz, 1H, H3), 4.11 (d, *J* = 4.0 Hz, 1H, H4), 4.06 (s, 2H, OCH_2), 3.76 (s, 3H, OCH_3), 3.03 (dd, *J* = 5.8 and 17.9 Hz 1H, $H6_{ax}$) and 2.90 (dd, *J* = 9.8 and 17.9 Hz, 1H, $H6_{eq}$) ppm. ^{13}C NMR (75 MHz, CD_3OD) δ: 167.8 (C), 140.4 (C), 137.9 (CH), 131.1 (C), 129.6 (2×CH), 129.6 (2×CH), 127.4 (CH), 124.2 (CH), 72.1 (CH), 67.0 (CH), 59.2 (OCH_3), 52.6 (CH), 32.6 (OCH_2) and 32.3 (CH_2) ppm. IR (ATR) υ: 3237 (OH) and 1716 (CO) cm^{-1}. MS (ESI) *m/z* = 330 (MH^+). HRMS calcd for $C_{17}H_{20}N_3O_4$ (MH^+): 330.1448; found, 330.1448.

(3*R*,4*S*,5*R*)-5-(4-benzyl-1*H*-1,2,3-triazol-1-yl)-3,4-dihydroxycyclohex-1-ene-1-carboxylic acid (4) – A solution of ester **15** (88.3 mg, 0.27 mmol) in THF (2.7 mL) was treated with an aqueous solution of lithium hydroxide (0.54 mL, 0.27 mmol, 0.5 M). The resulting mixture was stirred at room temperature for 30 min and then MilliQ water was added. The organic solvent was removed under reduced pressure and the resulting aqueous solution was washed with diethyl ether (×3). The aqueous layer was treated with Amberlite IR-120 (H^+) until pH 6. The filtrate and the washings were lyophilized to give the acid **4** (81.9 mg, 97%), as a white foam. $[\alpha]_D^{20} = -77.7^o$ (*c*1.3, MeOH). Mp: 152.0–153.5 ºC. ^{1}H NMR (500 MHz, CD_3OD) δ: 7.55 (br s, 1H, ArH), 7.22 (m, 4H, 4×ArH), 7.15 (m, 1H, ArH), 6.84 (br s, 1H, H2), 4.75 (m, 1H, H5), 4.28 (m, 1H, H3), 4.03 (d, *J* = 11.3 Hz, 1H, H4), 4.01 (s, 2H, OCH_2), 2.97 (dd, *J* = 4.5 and 17.7 Hz 1H, $H6_{ax}$) and 2.90 (dd, *J* = 10.2 and 17.7 Hz,

1H, $H6_{eq}$) ppm. ^{13}C NMR (125 MHz, CD_3OD) δ: 168.4 (C), 139.0 (C), 134.9 (CH), 128.3 (CH), 128.2 (3×CH), 126.1 (2×CH), 123.1 (C), 124.2 (CH), 72.1 (CH), 67.0 (CH), 59.2 (OCH_3), 52.6 (CH), 32.6 (CH_2) and 32.3 (CH_2) ppm. IR (ATR) υ: 3300 (OH) and 1710 (CO) cm^{-1}. MS (ESI) *m/z* = 314 (M–H). HRMS calcd for $C_{16}H_{16}N_3O_4$ (M–H): 314.1146; found, 314.1137.

Methyl (3*R*,4*S*,5*R*)-5-(4-phenoxymethyl-1*H*-1,2,3-triazol-1-yl)-3,4-dihydroxycyclohex-1-ene-1-carboxylate (16) – To a suspension of azide **14** (100 mg, 0.47 mmol) and 3-phenoxy-1-propine (0.06 mL, 0.47 mmol) in a 1:1 mixture of *t*-BuOH-water (2.4 mL) freshly prepared aqueous sodium ascorbate solution (0.47 mL, 1.0 M), followed by aqueous copper(II) sulphate solution (1.5 mL, 0.32 M) were added. The resultant heterogenous mixture was stirred vigorously during 16 h and then diluted with water and ethyl acetate. The organic layer was separated and the aqueous phase was extracted with ethyl acetate (×2). All the combined organic extracts were dried (anh. Na_2SO_4), filtered and evaporated. The obtained residue was purified by flash chromatography, eluting with (50:50) ethyl acetate/hexane, to afford triazol **16** (129 mg, 79%), as a white foam. $[\alpha]_D^{20} = -41.9^o$ (*c*1.3, MeOH). ^1H NMR (300 MHz, CD_3OD) δ: 7.83 (s, 1H, ArH), 6.98 (t, *J* = 8.0 Hz, 2H, 2×ArH), 6.66 (m, 3H, 3×ArH), 6.63 (s, 1H, H2), 4.59 (m, 1H, H5), 4.55 (s, 2H, OCH_2), 4.06 (t, *J* = 4.3 Hz, 1H, H3), 3.81 (dd, *J* = 4.1 and 10.8 Hz, 1H, H4), 3.46 (s, 3H, OCH_3), 2.75 (dd, *J* = 5.9 and 17.9 Hz 1H, $H6_{eq}$) and 2.63 (dd, *J* = 10.1 and 17.9 Hz, 1H, $H6_{ax}$) ppm. ^{13}C NMR (75 MHz, CD_3OD) δ: 167.8 (C), 159.8 (C), 144.5 (C), 137.9 (CH), 131.1 (C), 130.5 (2×CH), 125.7 (CH), 122.2 (CH), 115.8 (2×CH), 72.1 (CH), 66.7 (CH), 62.4 (OCH_2), 59.4 (CH), 52.6 (OCH_3) and 32.3 (CH_2) ppm. IR (ATR) υ: 3313 (OH) and 1722 (CO) cm^{-1}. MS (ESI) *m/z* = 346 (MH^+). HRMS calcd for $C_{17}H_{20}N_3O_5$ (MH^+): 346.1397; found, 346.1398.

(3*R*,4*S*,5*R*)-5-(4-phenoxymethyl-1*H*-1,2,3-triazol-1-yl)-3,4-dihydroxycyclohex-1-ene-1-carboxylic acid (5) – A solution of ester **16** (112.7 mg, 0.33 mmol) in THF (3.3 mL) was treated with an aqueous solution of lithium hydroxide (0.66 mL, 0.33 mmol, 0.5 M). The resulting mixture

was stirred at room temperature for 30 min and then MilliQ water was added. The organic solvent was removed under reduced pressure and the resulting aqueous solution was washed with diethyl ether (×3). The aqueous layer was treated with Amberlite IR-120 (H^+) until pH 6. The filtrate and the washings were lyophilized to give the acid **5** (104 mg, 95%), as a white foam. $[\alpha]_D^{20} = -77.2^o$ (*c*1.1, MeOH). ^{1}H NMR (500 MHz, CD_3OD) δ: 7.98 (s, 1H, ArH), 7.12 (t, *J* = 7.5 Hz, 2H, 2×ArH), 6.85 (d, *J* = 8.0 Hz, 2H, 2×ArH), 6.79 (t, *J* = 7.4 Hz, 1H, ArH), 6.64 (m, 1H, H2), 5.00 (s, 2H, OCH_2), 4.72 (dt, *J* = 5.8 and 10.8 Hz, 1H, H5), 4.20 (t, *J* = 4.6 Hz, 1H, H3), 3.97 (dd, *J* = 4.2 and 10.9 Hz, 1H, H4), 2.92 (dd, *J* = 5.7 and 17.9 Hz 1H, $H6_{eq}$) and 2.76 (ddd, *J* = 1.6, 10.6 and 17.9 Hz, 1H, $H6_{ax}$) ppm. ^{13}C NMR (75 MHz, CD_3OD) δ: 171.3 (C), 158.4 (C), 143.1 (C), 134.6 (C), 132.3 (CH), 129.2 (2×CH), 124.2 (CH), 120.9 (CH), 114.5 (2×CH), 71.2 (CH), 66.1 (CH), 61.0 (OCH_2), 58.6 (CH) and 32.4 (CH_2) ppm. IR (ATR) υ: 3407 (OH) and 1677 (CO) cm^{-1}. MS (ESI) *m/z* = 330 (M–H). HRMS calcd for $C_{16}H_{16}N_3O_5$ (M–H): 330.1095; found, 330.1090.

Methyl (3*S*,4*S*,5*R*)-3-amino-4-hydroxy-5-(naphth-2-yl)metoxycyclohex-1-ene-carboxylate (17h). A solution of alcohol **10h** (128 mg, 0.39 mmol) in dry tetrahydrofuran (3.5 mL), under inert atomosphere and at 0 ºC, was treated with triphenylphosphine (156 mg, 0.50 mmol), previously prepared hydrazoic acid[28] (0.45 mL, 0.59 mmol) and DIAD (0.12 mL, 0.59 mmol). The resulting solution was stirred at 0 ºC for 1.5 h and then the solvent was removed under reduced pressure. The resulting residue was purified by flash chromatography, eluting with (25:75) ethyl acetate/hexane. A solution of the resulting yellow oil (94 mg) in tetrahydrofuran (27 mL) and water (0.07 mL) was treated with triphenylphosphine (79.5 mg, 0.30 mmol) and then heated under reflux for 4 h. After cooling to room temperature, the solvent was removed under reduced pressure and the resulting residue was purified by flash chromatography, eluting with (10:90) methanol/dichlorometane, to give the amine **17h** (64 mg, 70%), as a yellow oil. $[\alpha]_D^{20} = -49.3^o$ (*c*1.1, $CHCl_3$). ^{1}H NMR (300 MHz, $CDCl_3$) δ: 7.82 (m, 4H, 4×ArH), 7.47 (d, *J* = 9.0 Hz, 3H, 3×ArH), 6.66 (br s, 1H, H2), 4.88 (d, *J* = 11.6 Hz, 3H, OC*H*H), 4.67 (d, *J* = 11.6 Hz, 3H, OCH*H*), 3.74 (s, 3H, OCH_3), 3.56 (m, 1H, H5), 3.43

(d, *J* = 5.8 Hz, 2H, H3+H4), 3.00 (dd, *J* = 5.4 and 17.3 Hz, 1H, $H6_{ax}$), 2.35 (br s, 3H, OH+NH_2) and 2.28–2.15 (m, 1H, $H6_{eq}$) ppm. ^{13}C NMR (100 MHz, $CDCl_3$) δ: 166.8 (C), 140.4 (CH), 135.4 (C), 133.3 (C), 133.1 (C), 128.5 (CH), 127.9 (CH), 127.8 (CH), 127.4 (C), 126.8 (CH), 126.3 (CH), 126.1 (CH), 125.9 (CH), 77.0 (2×CH), 71.5 (OCH_2), 54.4 (CH), 52.1 (OCH_3) and 29.8 (CH_3) ppm. IR (ATR) υ: 3313 (NH), 3281 (OH) and 1716 (CO) cm^{-1}. MS (ESI) *m/z* = 328 (MH^+). HRMS calcd for $C_{19}H_{22}NO_4$ (MH^+): 328.1543; found, 328.1547.

Sodium (3*S*,4*S*,5*R*)-3-amino-4-hydroxy-5-(naphth-2-yl)metoxycyclohex-1-ene-carboxylate (6h). A solution of ester **17h** (58 mg, 0.18 mmol) in THF (1.8 mL) was treated with an aqueous solution of sodium hydroxide (0.36 mL, 0.5 M). The resulting mixture was stirred at room temperature for 30 min and then MilliQ water was added. The organic solvent was removed under reduced pressure and the resulting aqueous solution was washed with diethyl ether (×2) and lyophilized to give the sodium salt **6h** (54 mg, 93%), as a yellow foam. $[\alpha]_D^{20} = -14.5^o$ (*c*0.9, H_2O). ^{1}H NMR (500 MHz, D_2O) δ: 7.88 (m, 3H, 3×ArH), 7.85 (br s, 1H, ArH), 7.51 (m, 3H, 3×ArH), 6.17 (br s, 1H, H2), 4.78 (d, *J* = 11.7 Hz, 1H, OC*H*H), 4.71 (d, *J* = 11.7 Hz, 1H, OCH*H*), 3.57 (td, *J* = 5.8 and 9.5 Hz, 1H, H5), 3.40 (t, *J* = 8.9 Hz, 1H, H4), 3.28 (m, 1H, H3), 2.80 (dd, *J* = 5.7 and 17.2 Hz, 1H, $H6_{ax}$) and 2.18–2.11 (m, 1H, $H6_{eq}$) ppm. ^{13}C NMR (125 MHz, D_2O) δ: 175.2 (C), 135.3 (C), 133.7 (CH), 132.8 (2×C), 132.7 (C), 128.2 (CH), 127.8 (CH), 127.6 (CH), 127.1 (CH), 126.5 (CH), 126.4 (2×CH), 77.3 (CH), 76.2 (CH), 71.5 (OCH_2), 55.5 (CH) and 31.0 (CH_2) ppm. IR (ATR) υ: 3326 (NH+OH) and 1551 (CO) cm^{-1}. MS (ESI) *m/z* = 336 (MH^+). HRMS calcd for $C_{18}H_{19}NNaO_4$ (MH^+): 336.1206; found, 336.1199.

Methyl (3*S*,4*S*,5*R*)-3-amino-5-(benzo[*b*]thiophen-5-yl)methoxy-4-hydroxycyclohex-1-ene-carboxylate (17i). A solution of alcohol **10i** (124.5 mg, 0.37 mmol) in dry tetrahydrofuran (3.4 mL), under inert atomosphere and at 0 ºC, was treated with triphenylphosphine (148.4 mg, 0.56 mmol), previously prepared hydrazoic acid (0.43 mL, 0.56 mmol) and DIAD (0.11 mL, 0.56 mmol). The resulting solution was stirred at 0 ºC for 1.5 h and then the solvent was removed under reduced

pressure. The resulting residue was purified by flash chromatography, eluting with (25:75) ethyl acetate/hexane. A solution of the resulting yellow oil (107 mg) in tetrahydrofuran (30 mL) and water (0.07 mL) was treated with triphenylphosphine (87 mg, 0.33 mmol) and then heated under reflux for 4 h. After cooling to room temperature, the solvent was removed under reduced pressure and the resulting residue was purified by flash chromatography, eluting with (10:90) methanol/dichlorometane, to give the amine **10i** (71.8 mg, 70%), as a yellow oil. $[\alpha]_D^{20}$ = –47.4º (*c*1.0, $CHCl_3$). ^{1}H NMR (300 MHz, $CDCl_3$) δ: 7.82 (d, *J* = 8.2 Hz, 1H, ArH), 7.76 (br s, 1H, ArH), 7.42 (d, *J* = 4.7 Hz, 1H, ArH), 7.29 (m, 2H, 2×ArH), 6.63 (br s, 1H, H2), 4.81 (d, *J* = 11.3 Hz, 1H, OC*H*H), 4.60 (d, *J* = 11.3 Hz, 1H, OCH*H*), 3.72 (s, 3H, OCH_3), 3.51 (m, 1H, H5), 3.38 (br s, 2H, H3+H4), 2.95 (dd, *J* = 5.3 and 17.3 Hz, 1H, $H6_{ax}$), 2.44 (br s, 3H, OH+NH_2) and 2.19 (m, 1H, $H6_{eq}$) ppm. ^{13}C NMR (63 MHz, $CDCl_3$) δ: 166.7 (C), 140.3 (CH), 139.7 (C), 139.3 (C), 134.1 (CH), 127.3 (2×C), 127.3 (CH), 124.4 (CH), 123.8 (CH), 123.0 (CH), 122.6 (CH), 76.9 (CH), 76.6 (CH), 71.4 (OCH_2), 54.2 (CH), 52.0 (OCH_3) and 29.8 (CH_2) ppm. IR (ATR) υ: 3065 (NH+OH) and 1716 (CO) cm^{-1}. MS (ESI) *m/z* = 334 (MH^+). HRMS calcd for $C_{17}H_{20}NSO_4$ (MH^+): 334.1108; found, 334.1113.

Sodium (3*S*,4*R*,5*R*)-3-amino-5-(benzo[*b*]thiophen-5-yl)methoxy-4-hydroxycyclohex-1-ene-carboxylate (6i). A solution of ester **17i** (68.1 mg, 0.18 mmol) in THF (2 mL) was treated with an aqueous solution of sodium hydroxide (0.4 mL, 0.5 M). The resulting mixture was stirred at room temperature for 30 min and then MilliQ water was added. The organic solvent was removed under reduced pressure and the resulting aqueous solution was washed with diethyl ether (×2) and lyophilized to give the sodium salt **6i** (62 mg, 91%), as a yellow foam. $[\alpha]_D^{20}$ = –19.6º (*c*1.0, H_2O). ^{1}H NMR (500 MHz, D_2O) δ: 7.60 (d, *J* = 8.1 Hz, 1H, ArH), 7.53 (br s, 1H, ArH), 7.28 (d, *J* = 4.8 Hz, 1H, ArH), 7.11 (m, 1H, ArH), 6.13 (br s, 1H, H2), 4.46 (d, *J* = 11.5 Hz, 1H, OC*H*H), 4.38 (d, *J* = 11.5 Hz, 1H, OCH*H*), 3.27 (br s, 2H, H5+H4), 3.11 (br s, 1H, H3), 2.67 (d, *J* = 15.9 Hz, 1H, $H6_{ax}$) and 2.06 (m, 1H, $H6_{eq}$) ppm. ^{13}C NMR (125 MHz, D_2O) δ: 174.9 (C), 139.5 (C), 138.9 (C), 133.8 (CH+C), 132.8 (C), 127.4 (CH), 124.6 (CH), 123.9 (CH), 123.2 (CH), 122.5 (CH), 77.1 (CH), 76.1

(CH), 71.3 (OCH_2), 53.4 (CH) and 31.0 (CH_2) ppm. IR (ATR) υ: 3332 (NH+OH) and 1551 (CO) cm^{-1}. MS (ESI) *m/z* = 342 (MH^+). HRMS calcd for $C_{16}H_{17}NSNaO_4$ (MH^+): 342.0770; found, 342.0769.

Shikimate kinase assay – Both enzymes were purified as described previously.[30,18] The *H. pylori* enzyme used in these studies was expressed and produced using genomic DNA from an isolated clinical strain, courtesy of Guadalajara Hospital (Guadalajara, Spain). Concentrated solutions of *Hp*-SK (7.4 mg mL^{-1}) or *Mt*-SK (1.5 mg mL^{-1}) were stored in potassium phosphate buffer (50 mM, pH 7.2), DTT (1 mM) and NaCl (150 mM). When required for assays, aliquots of the enzyme stock solutions were diluted in water and buffer and stored on ice. Enzyme activity was measured by monitoring the decrease in absorbance at 340 nm in the UV spectrum due to the absorbance of NADH (ε/M^{-1} cm^{-1} 6 220) in a coupled assay format wherein ADP formed after the formation of shikimate-3-phosphate (**2**) was detected using pyruvate kinase (PK) and lactate dehydrogenase (LDH). Oxidation of NADH to NAD during PK-LDH activity was monitored at 340 nm. Standard assay conditions for shikimate kinase were 100 mM Tris.HCl pH 7.7, 100 mM NaCl, 5 mM $MgCl_2$, 2.5 mM ATP, 1 mM shikimic acid (**1**), 0.20 mM NADH, ~2.8 units of PK-LDH and 0.03 unit of SK protein. One unit of enzyme is defined as the amount of enzyme required to convert 1 µmol of substrate to product in 1 min. Each assay was initiated by addition of shikimic acid (**1**). Solutions of ATP (ε/M^{-1} cm^{-1} 15 400) and NADH were calibrated by measuring the absorbance at 259 nm and 340 nm in the UV spectrum, respectively. Solutions of shikimic acid (**1**) were calibrated by equilibration with SK and measurement of the change in the UV absorbance at 340 nm due to the disappearance of NADH. The K_i values of compounds **3–6** against SK were obtained from Dixon plots (1/v *vs* [I]) of assay data. The initial rates at fixed enzyme and substrate concentrations (0.25–1.4 K_m) were measured in the absence and in the presence of various inhibitor concentrations. The determined kinetic parameters for *Hp*-SK and *Mt*-SK were K_m (**1**) = 39 ± 8 µM; k_{cat} = 116 ± 4 10^{-3} s^{-1} and K_m (**1**) = 544 ± 14 µM; k_{cat} = 295 ± 8 s^{-1}, respectively.

Susceptibility testing – A *H. pylori* clinical isolate obtained from a biopsy of a patient of the Guadalajara Hospital (Guadalajara, Spain) was employed. The clinical strain was cultured on plates of Trypticase soy agar with 10% sheep blood and was incubated under microaerophilic conditions (5% O_2, 10% CO_2, 85% N_2) for 5–6 days. The strain was stored at –80°C in Luria-Bertani medium with 20% of glicerol until use. The agar dilution method was used to determine the Minimum Inhibitory Concentration (MICs) of the compounds, according to the standard method recommended by CLSI.[27] The suspension turbidity used to inoculate the plates was adjusted to a McFarland opacity standard of 2.0. Then 10 µL of the bacterial suspension were dropped in plates of Trypticase soy agar with 10% sheep blood. The plates contained 2-fold dilutions of each compound with concentrations ranging from 4 to 1028 µg/mL. The MICs were determined after 6 days of incubation at 37°C under microaerophilic conditions. MIC values were defined as the lowest concentration of each compound that completely inhibited visible growth on plates. MIC assays were performed at least three times.

Docking studies – These studies were carried out using the GOLD 5.2[20] program and the enzyme coordinates collected in the MD simulation studies carried out with the SK complex containing: (a) *Mt*-SK/ATP/Mg^{+2}/(6*R*)-6-hydroxyshikimic acid (10 ns)[18]; (b) *Hp*-SK/ADP/**2** (50 ns). Different snapshots of the simulation were selected, specifically, those ones in which a large movement in the α-helices α2 and α3 of the SB domain was observed. Experimental details of the MD simulation studies are described in the next section. The best results were obtained after 7 ns of MD for *Mt*-SK and 11 ns for *Hp*-SK. Water molecules were removed from the model. Ligand geometries were minimized using the AM1 Hamiltonian as implemented in the program Gaussian 09[31] and these were used as MOL2 files. Each ligand was docked in 25 independent genetic algorithm (GA) runs, and for each of these a maximum number of 100000 GA operations were performed on a single population of 50 individuals. Operator weights for crossover, mutation and migration in the entry box were used as default parameters (95, 95, and 10, respectively) along with the hydrogen bonding (4.0 Å) and van der Waals (2.5 Å) parameters. The position of (6*R*)-6-hydroxyshikimic acid and **2** in the

corresponding model was used to define the active-site and the radius was set to 7 Å. The "flip ring corners" flag was switched on, while all the other flags were off. The GOLD scoring function was used to rank the ligands in order of fitness.

Molecular dynamics simulations – *Ligand minimization*. Ligand geometries were minimized using a restricted Hartree–Fock (RHF) method and a 6–31G(d) basis set, as implemented in the *ab initio* program Gaussian 09. The resulting wavefunctions were used to calculate electrostatic potential-derived (ESP) charges employing the restrained electrostatic potential (RESP)[21] methodology, as implemented in the assisted model building with energy refinement (AMBER)[32] suite of programs. The missing bonded and non-bonded parameters were assigned, by analogy or through interpolation, from those already present in the AMBER database (GAFF).[31,33]

Generation and minimization of ternary complexes. Simulations of (6*R*)-6-hydroxyshikimic acid/ATP/SK complex were carried out as previously described MD simulation of the Michaelis complex *Mt*-SK/ATP/**1**[18] after manual replacement of shikimic acid (**1**) by (6*R*)-6-hydroxyshikimic acid. Simulations of *Hp*-SK/ADP/**2** complex were performed using the enzyme geometries found in the crystal structure of *Hp*-SK in complex with ADP and **2** (PDB code 3MUF[19]). Simulations of inhibitor/ATP/SK complexes were carried out using the highest score solution obtained by docking and the enzyme geometries used in those docking studies, as described above. Computation of the protonation state of titratable groups at pH 7.0 was carried out using the H^{++} Web server.[34] Addition of hydrogen and molecular mechanics parameters from the ff03 and GAFF force fields, respectively, were assigned to the protein and the ligands using the LEaP module of AMBER Tools 14.[32,33,35] ATP, ADP and Mg^{2+} parameters used with the AMBER force field were included.[36,37]

All systems were minimized in four stages: (a) initial minimization of the ligand and the closest residues of the SB domain (500 steps, first half using steepest descent and the rest using conjugate gradient); (b) minimization of the solvent and ions (5000 steps, first half using steepest descent and the rest using conjugate gradient); (c) minimization of the side chains, waters and ions (5000 steps,

first half using steepest descent and the rest using conjugate gradient); (d) final minimization of the whole system (5000 steps, first half using steepest descent and the rest using conjugate gradient). A positional restraint force of 50 kcal mol^{-1} $Å^{-2}$ was applied to those unminimized atoms during the first three stages (a–c). The complex was immersed in a truncated octahedron of ~5200 TIP3P water molecules and neutralized by addition of chloride (*Mt*-SK) or sodium (*Hp*-SK) ions.[32,38,39]

Simulations. MD simulations were performed using the sander module from the AMBER 12 suite of programs. Periodic boundary conditions were applied and electrostatic interactions were treated using the smooth particle mesh Ewald method (PME)[40] with a grid spacing of 1 Å. The cutoff distance for the non-bonded interactions was 9 Å. The SHAKE algorithm[41] was applied to all bonds containing hydrogen, using a tolerance of 10^{-5} Å and an integration step of 2.0 fs. Minimization was carried out in three steps, starting with the octahedron water hydrogens, followed by solvent molecules and counterions, and finally the entire system. The minimized system was then heated at 300 K at 1 atm by increasing the temperature from 0 K to 300 K over 100 ps and by keeping the system at 300 K another 100 ps. A positional restraint force of 50 kcal mol^{-1} $Å^{-2}$ was applied to all α carbons during the heating stage. Finally, an equilibration of the system at constant volume (100 ps with positional restraints of 5 kcal mol^{-1} $Å^{-2}$ to α alpha carbons) and constant pressure (another 100 ps with positional restraints of 5 kcal mol^{-1} $Å^{-2}$ to α alpha carbons) were performed. The positional restraints were gradually reduced from 5 to 1 mol^{-1} $Å^{-2}$ (5 steps, 100 ps each), and the resulting systems were allowed to equilibrate further (100 ps). Unrestrained MD simulations were carried out for 50 ns. System coordinates were collected every 10 ps for further analysis. Figures depicting structures were prepared using PYMOL.[42]

AUTHOR INFORMATION

Corresponding Author

concepcion.gonzalez.bello@usc.es; Phone: +34 881 815726.

Notes

The authors declare no competing financial interests.

Funding Sources

Financial support from the Spanish Ministry of Economy and Competiveness (SAF2013-42899-R), Xunta de Galicia (GRC2013-041) and the European Regional Development Fund (ERDF) is gratefully acknowledged. VP and MM thank the Spanish Ministry of Economy and Competiveness and the Spanish Ministry of Education for their respective FPI and FPU fellowships. EL thanks the Xunta de Galicia for his postdoctoral fellowship. JCV-U and AB thank the Miguel Servet Programme ISCIII-FEDER (CP13/00226) and the ISCIII General Subdirection of Assesment and Promotion of the Research (PI14/00059) for financial support.

ACKNOWLEDGMENT

We are grateful to the Centro de Supercomputación de Galicia (CESGA) for use of the Finis Terrae computer and Dr. Trinidad Parra Cid from Guadalajara Hospital (Guadalajara, Spain) for kindly providing the *Helicobacter pylori* clinical isolate.

ABBREVIATIONS USED

SK, Shikimate kinase; *Mt*-SK, Shikimate kinase from *Mycobacterium tuberculosis*; *Hp*-SK, Shikimate kinase from *Helicobacter pylori*; MD, molecular dynamics; SB, substrate binding; PDB, protein data bank. GB, generalized Born.

REFERENCES

(1) Wright, G. D. The antibiotic resistome: the nexus of chemical and genetic diversity. *Nature Rev. Microbiol.* **2007**, *5*, 175–186.

(2) Bush, K. Investigational agents for the treatment of Gram-negative bacterial infections: a reality check. *ACS Infect. Dis.* **2015**, *1*, 509–511.

(3) Brown, D. Antibiotic resistance breakers: can repurposed drugs fill the antibiotic discovery avoid?. *Nature Rev. Drug Discov.* **2015**, *14*, 821–832.

(4) Wright, G. D. Antibiotics: a new hope. *Chem. Biol.* **2012**, *19*, 3–10.

(5) Brown, E. D.; Wright, G. D. Antibacterial drug discovery in the resistance era. *Nature* **2016**, *529*, 336–343.

(6) Fair, R. J.; Tor, Y. Antibiotics and bacterial resistance in the 21st century. *Perspect. Medicin. Chem.* **2014**, *6*, 25–64.

(7) Chellat, M. F.; Raguž, L.; Riedl, R. Targeting antibiotic resistance. *Angew. Chem. Int. Ed.* **2016**, *55*, 22-30.

(8) D`Costa, V. M.; King, C. E.; Kalan, L.; Morar, M.; Sung, W. W. L.; Schwarz, C.; Froese, D.; Zazula, G.; Calmels, F.; Debruyne, R.; Golding, G. B.; Poinar, H. N.; Wright, G. D. Antibiotic resistance is ancient. *Nature* **2011**, *477*, 457–461.

(9) González-Bello, C. Inhibition of shikimate kinase and type II dehydroquinase for antibiotic discovery: structure-based design and simulation studies. *Curr. Top. Med. Chem.* **2016**, *16*, 960–977.

(10) Abell, C. Enzymology and Molecular Biology of the Shikimate Pathway, In: *Comprehensive Natural Products Chemistry*; Sankawa, U. Ed.; Pergamon, Elsevier Science Ltd.: Oxford, **1999**; Vol 1, pp. 573–607.

(11) Lamichhane, G.; Freundlich, J. S.; Ekins, S.; Wickramaratne, N.; Nolan, S. T.; Bisha, W. R. Essential metabolites of *Mycobacterium tuberculosis* and their mimics. *mBio* **2011**, *2*, e00301–e00310.

(12) (a) Data base for essential genes in bacteria see www.essentialgene.org (accessed March 1, 2016). (b) Zhang, R.; Ou, H.-Y.; Zhang, C.-T. DEG, a database of essential genes. *Nucleic Acids Res.* **2004**, *32*, D271–D272. (c) Zhang, R.; Lin, Y. DEG 5.0, a database of essential genes in both prokaryotes and eukaryotes. *Nucleic Acids Res.* **2009**, *37*, D455–D458.

(13) Simithy, J.; Reeve, N.; Hobrath, J. V.; Reynolds, R. C. Identification of shikimate kinase inhibitors among anti-Mycobacterium tuberculosis compounds by LC-MS. *Tuberculosis* **2014**, *94*, 152–158.

(14) Han, C.; Zhang, J.; Chen, L.; Chen, K.; Shen, X.; Jiang, H. Discovery of *Helicobacter pylori* shikimate kinase inhibitors: bioassay and molecular modeling. *Bioorg. Med. Chem.* **2007**, *15*, 656–662.

(15) Prado, V.; Lence, E.; Vallejo, J. A.; Beceiro, A.; Thompson, P.; Hawkins, A. R.; González-Bello, C. Study of the phosphoryl-transfer mechanism of shikimate kinase by NMR spectroscopy. *Chem. Eur. J.* **2016**, *22*, 2758–2768.

(16) Hartmann, M. D.; Bourenkov, G. P.; Oberschall, A.; Strizhov, N.; Bartunik, H. D. Mechanism of phosphoryl transfer catalyzed by shikimate kinase from *Mycobacterium tuberculosis. J. Mol. Biol.* **2006**, *364*, 411–423.

(17) Cheng, W.-C.; Chang, Y.-N.; Wang, W.-C. Structural basis for shikimate-binding specificity of *Helicobacter pylori* shikimate kinase. *J. Bacteriol*. **2005**, *187*, 8156–8163.

(18) Blanco, B.; Prado, V.; Lence, E.; Otero, J. M.; García-Doval, C.; van Raaij, M. J.; Llamas-Saiz, A. L.; Lamb, H.; Hawkins, A. R.; González-Bello, C. *Mycobacterium tuberculosis* shikimate kinase inhibitors: design and simulation studies of the catalytic turnover. *J. Am. Chem. Soc*. **2013**, *135*, 12366–12376.

(19) Cheng, W.-C.; Chen, Y.-F.; Wang, H.-J.; Hsu, K.-C.; Lin, S.-C.; Chen, T.-J.; Yang, J.-M., Wang, W.-C. Structures of *Helicobacter pylori* shikimate kinase reveal a selective inhibitor-induced-fit mechanism. *PLoS ONE* **2012**, *7*, e33481.

(20) http://www.ccdc.cam.ac.uk/products/life_sciencies/gold/ (accessed March 1, 2016).

(21) (a) Cornell, W. D.; Cieplak, P.; Bayly, C. I.; Gould, I. R.; Merz, K. M.; Ferguson, D. M.; Spellmeyer, D. C.; Fox, T.; Caldwell, J. W.; Kollman, P. A. A second generation force field for

the simulation of proteins, nucleic acids, and organic molecules. *J. Am. Chem. Soc.* **1995**, *117*, 5179−5197. (b) http://q4md-forcedfieldtools.org/RED/resp/ (accessed March 1, 2016).

(22) Bianco, A.; Brufani, M.; Manna, F.; Melchioni, C. Synthesis of a carbocyclic sialic acid analogue for the inhibition of influenza virus neuraminidase. *Carbohydrate Research* **2001**, *332*, 23–31.

(23) Pansegrau, P. D.; Anderson, K. S.; Widlanski, T.; Ream, J. E.; Sammons, R. D.; Sikorski, J. A.; Knowles, J. R. Synthesis and evaluation of two inhibitors of EPSP synthase. *Tetrahedron Lett.* **1991**, *32*, 2589–2592.

(24) Meier, R. M.; Tamm, C. Studies direct towards the biosynthesis of the C7N unit of rifamycin B: a new synthesis of quinic acid from shikimic acid. *Helv. Chim. Acta* **1991**, 74, 807–818.

(25) McGowan, D. A.; Berchtold, G. A. (-)-Methyl cis-3-hydroxy-4,5-oxycyclohex-1-enecarboxylate: stereospecific formation from and conversion to (-)-methyl shikimate; complex formation with bis(carbomethoxy)hydrazine. *J. Org. Chem.* **1981**, *46*, 2381−2383.

(26) Tizón, L.; Otero, J. M.; Prazeres, V. F. V.; Llamas-Saíz, A. L.; van Raaij, M. J.; Lamb, H.; Hawkins, A. R.; Ainsa, J. A.; Castedo, L.; González-Bello, C. A prodrug approach for improving anti-tuberculosis activity of potent *Mycobacterium tuberculosis* type II dehydroquinase inhibitors. *J. Med. Chem.* **2011**, *54*, 6063–6084.

(27) Clinical and Laboratory Standards Institute. Performance Standards for Antimicrobial Susceptibility Testing: Seventeenth Informational Supplement M100-S17. Wayne, PA, USA: CLSI; 2007.

(28) Miller III, B. R.; McGee Jr., T. D.; Swails, J. M.; Homeyer, N.; Gohlke, H.; Roitberg, A. E. MMPBSA.py: an efficient program for end-state free energy calculations. *J. Chem. Theory Comput.* **2012**, *8*, 3314−3321.

(29) Marchini, M.; Mingozzi, M.; Colombo, R.; Guzzetti, I.; Belvisi, L.; Vasile, F.; Potenza, D.; Piarulli, U.; Arosio, D.; Gennari, C. Cyclic RGD peptidomimetics containing bifunctional diketopiperazine scaffolds as new potent integrin ligands. *Chem. Eur. J.* **2012**, *18*, 6195–6207.

(30) Krell, T.; Maclean, J.; Boam, D. J.; Cooper, A.; Resmini, M.; Brocklehurst, K.; Kelly, S. M.; Price, N. C.; Lapthorn, A. J.; Coggins, J. R. Biochemical and X-ray crystallographic studies on shikimate kinase: The important structural role of the P-loop lysine. *Protein Science* **2001**, *10*, 1137–1149.

(31) Frisch, M. J.; Trucks, G. W.; Schlegel, H. B.; Scuseria, G. E.; Robb, M. A.; Cheeseman, J. R.; Scalmani, G.; Barone, V.; Mennucci, B.; Petersson, G. A.; Nakatsuji, H.; Caricato, M.; Li, X.; Hratchian, H. P.; Izmaylov, A. F.; Bloino, J.; Zheng, G.; Sonnenberg, J. L.; Hada, M.; Ehara, M.; Toyota, K.; Fukuda, R.; Hasegawa, J.; Ishida, M.; Nakajima, T.; Honda, Y.; Kitao, O.; Nakai, H.; Vreven, T.; Montgomery, Jr. J. A.; Peralta, J. E.; Ogliaro, F.; Bearpark, M.; Heyd, J. J.; Brothers, E.; Kudin, K. N.; Staroverov, V. N.; Kobayashi, R.; Normand, J.; Raghavachari, K.; Rendell, A.; Burant, J. C.; Iyengar, S. S.; Tomasi, J.; Cossi, M.; Rega, N.; Millam, J. M.; Klene, M.; Knox, J. E.; Cross, J. B.; Bakken, V.; Adamo, C.; Jaramillo, J.; Gomperts, R.; Stratmann, R. E.; Yazyev, O.; Austin, A. J.; Cammi, R.; Pomelli, C.; Ochterski, J. W.; Martin, R. L.; Morokuma, K.; Zakrzewski, V. G.; Voth, G. A.; Salvador, P.; Dannenberg, J. J.; Dapprich, S.; Daniels, A. D.; Farkas, Ö.; Foresman, J. B.; Ortiz, J. V.; Cioslowski, J.; Fox, D. J. Revision D.01, Gaussian, Inc., Wallingford CT, **2009**.

(32) Case, D. A.; Cheatham, T. E.; Darden, T.; Gohlke, H., Luo, R.; Merz, K. M.; Onufriev, O.; Simmerling, C.; Wang, B.; Woods, R. J. The AMBER biomolecular simulation program. *J. Comput. Chem.* **2005**, *26*, 1668–1688.

(33) (a) Wang, J.; Wolf, R. M.; Caldwell, J. W.; Kollman, P. A.; Case, D. A. Development and testing of a general amber force field. *J. Comp. Chem.* **2004**, *25*, 1157–1174. (b) Wang, J.;

Wang, W.; Kollman, P. A.; Case, D. A. Automatic atom type and bond type perception in molecular mechanical calculations. *J. Mol. Graphics Modell.* **2006**, *25*, 247−260.

(34) (a) Gordon, J. C.; Myers, J. B.; Folta, T.; Shoja, V.; Heath, L. S.; Onufriev, A. *Nucleic Acids Res* **2005**, *33* (Web Server issue):W368−371. (b) http://biophysics.cs.vt.edu/H++ (accessed March 1, 2016).

(35) Amber Tools 1.5: Case, D. A.; Berryman, J. T.; Betz, R.M.; Cerutti, D.S.; Cheatham III, T. E.; Darden, T. A.; Duke, R. E.; Giese, T. J.; Gohlke, H.; Goetz, A.W.; Homeyer, N.; Izadi, S.; Janowski, P.; Kaus, J.; Kovalenko, A.; Lee, T. S.; LeGrand, S.; Li, P.; Luchko, T.; Luo, R.; Madej, B.; Merz, K. M.; Monard, G.; Needham, P.; Nguyen, H.; Nguyen, H. T.; Omelyan, I.; Onufriev, A.; Roe, D. R.; Roitberg, A.; Salomon-Ferrer, R.; Simmerling, C. L.; Smith, W.; Swails, J.; Walker, R. C.; Wang, J.; Wolf, R. M.; Wu, X.; York, D. M.; Kollman, P.A. AMBER 2015, University of California, San Francisco, 2015.

(36) Mg^{2+} parameters used with the AMBER force field were downloaded from http://www.pharmacy.manchester.ac.uk/bryce/amber/ (accessed March 1, 2016). Allnér, O.; Nilsson, L.; Villa, A. Magnesium ion–water coordination and exchange in biomolecular simulations. *J. Chem. Theory Comput.* **2012**, 8, 1493–1502.

(37) ATP and ADP parameters used with the AMBER force field were downloaded from http://www.pharmacy.manchester.ac.uk/bryce/amber/ (accessed March 1, 2016). Meagher, K. L.; Redman, L. T.; Carlson, H. A. Development of polyphosphate parameters for use with the AMBER force field. *J. Comput. Chem.* **2003**, *24*, 1016−1025.

(38) Aqvist, J. Ion-water interaction potentials derived from free energy perturbation simulations. *J. Phys. Chem.* **1990**, *94*, 8021–8024.

(39) Jorgensen, W. L.; Chandrasekhar, J.; Madura, J. D. Temperature and size dependence for Monte Carlo simulations of TIP4P water. *J. Chem. Phys.* **1983**, *79*, 926–935.

(40) Darden, T. A.; York, D.; Pedersen, L. G. Particle mesh Ewald: An W log(N) method for Ewald sums in large systems. *J. Chem. Phys.* **1993**, *98*, 10089–10092.

(41) Ryckaert, J.-P.; Ciccotti, G.; Berendsen, H. J. C. Numerical integration of the cartesian equations of motion of a system with constraints: molecular dynamics of n-alkanes. *J. Comput. Phys.* **1977**, *23*, 327–341.

(42) DeLano, W.L. The PyMOL Molecular Graphics System. (2008) DeLano Scientific LLC, Palo Alto, CA, USA. http://www.pymol.org/ (accessed March 1, 2016).

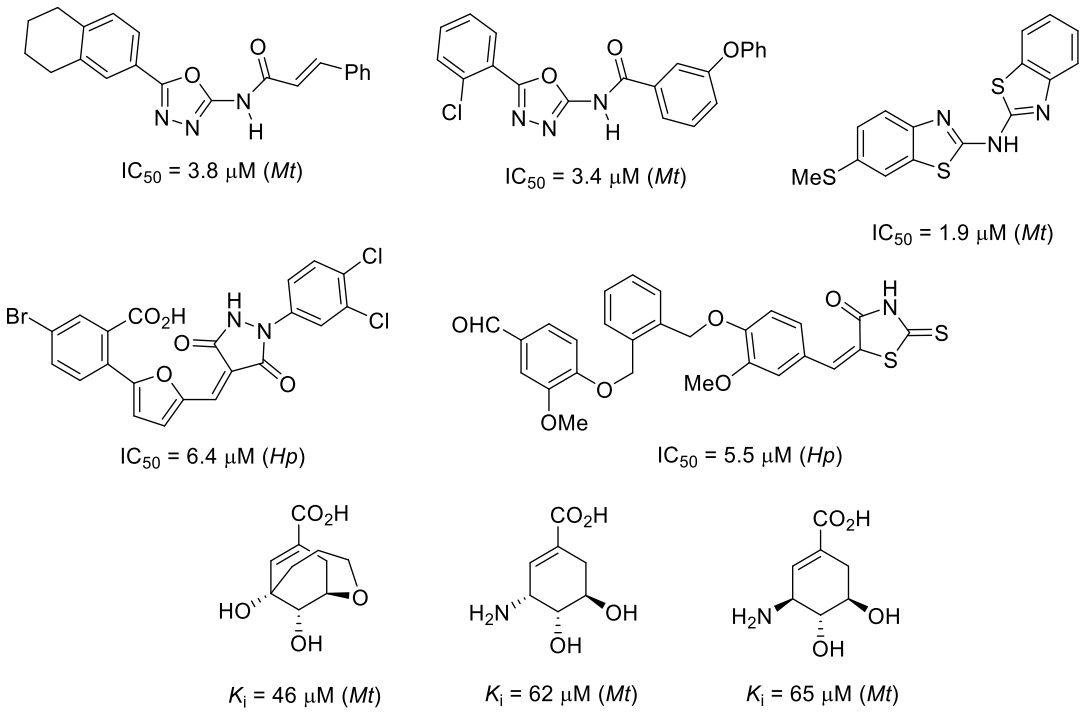

Figure 1. Selected examples of SK inhibitors identified by screening[13,14] and by structure-based[18] desing. The reported IC_{50} and K_i values for *Mt*-SK and *Hp*-SK are included.

Scheme 1. Enzymatic conversion catalyzed by the SK enzyme.

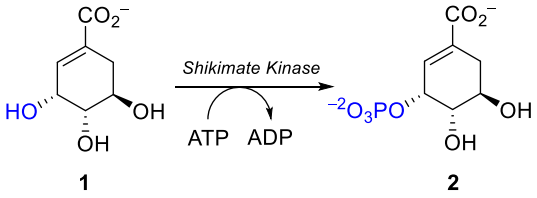

1 **2**

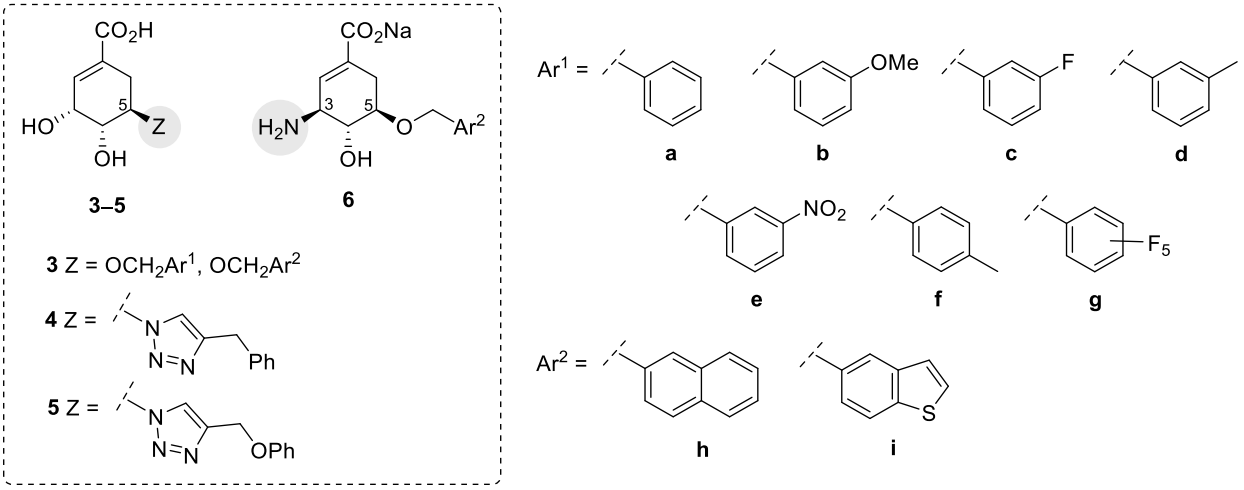

Figure 2. Target compounds **3**–**6**.

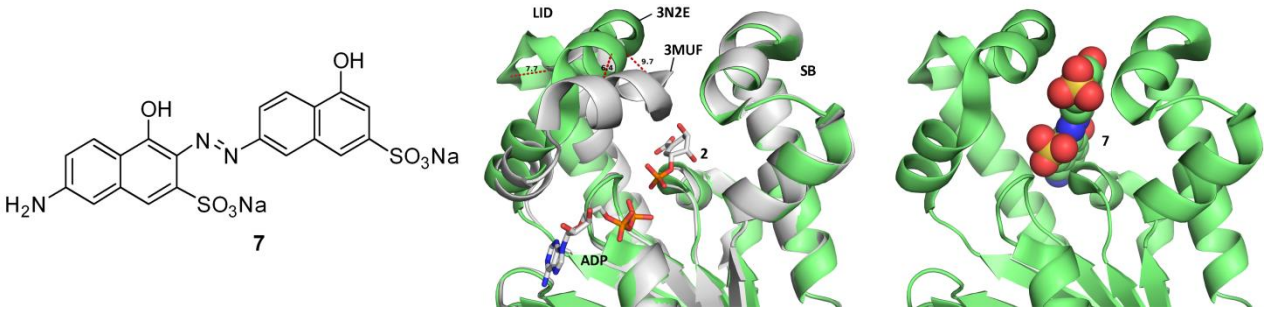

Figure 3. Comparison of the complexes *Hp*-SK/ADP/**2** (PDB entry 3MUF, 2.3 Å, gray) *vs* E114A *Hp*-SK/**7** (PDB entry 3N2E, 2.53 Å, green). Note the large conformational change of the LID domain caused by compound **7** (up to 9.7 Å).

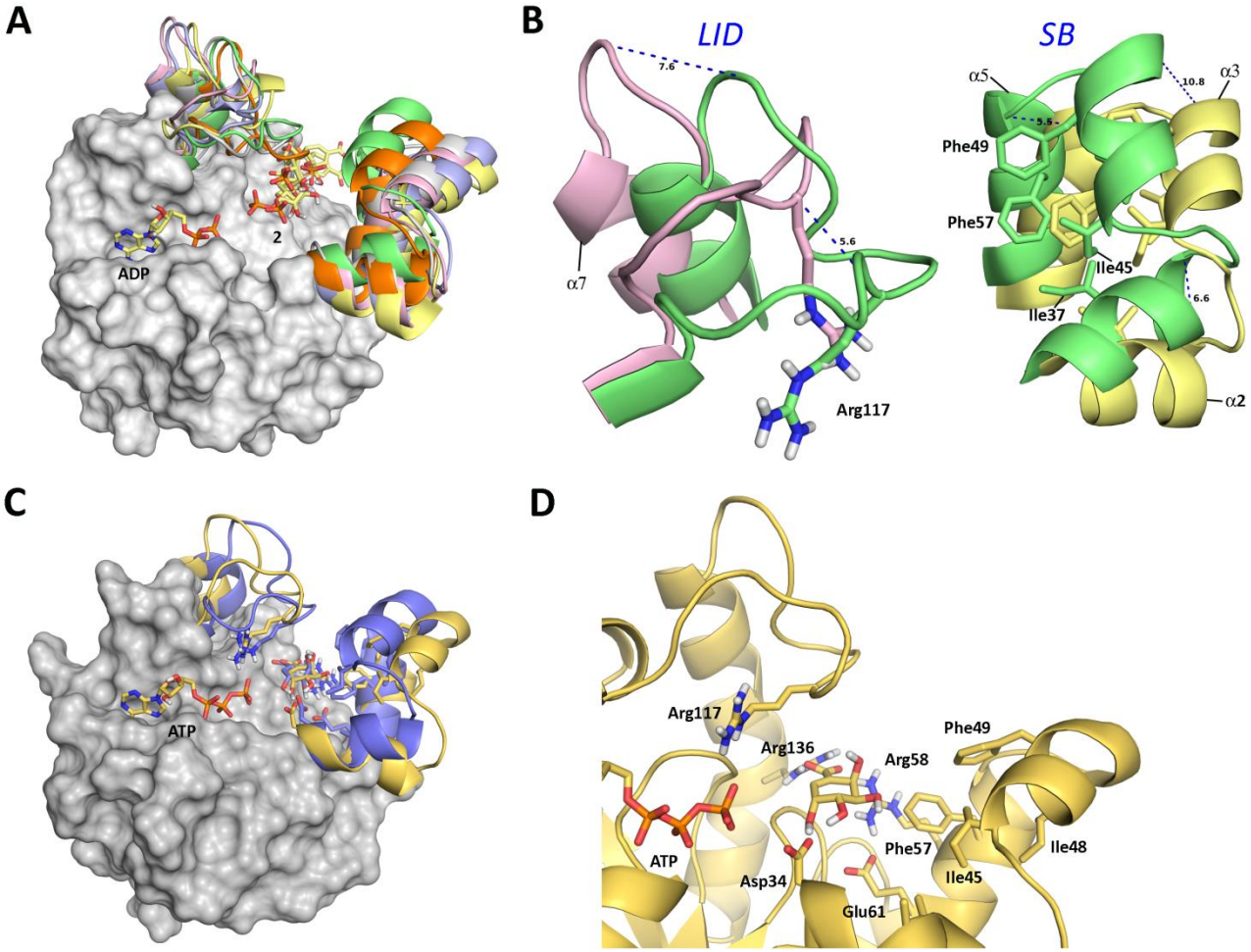

Figure 4. (A) Overall view of the *Mt*-SK motion required for product release from the active site obtained by MD simulations. (B) Detail of the large conformational changes of the LID and the α-helices α2, α3 and α5 of the SB domains during 10 ns of simulation. The arrangement of the most open/closed conformations of the LID and SB domains are shown. (C) Conformational changes of the LID and SB domains of *Mt*-SK caused by the binding mode of (6*R*)-6-hydroxyshikimic acid obtained by MD simulations. Comparison of the arrangement of those domains after minimization and prior simulation (blue) and after 7 ns of simulation (yellow) is shown. (D) Detail of the binding mode of (6*R*)-6-hydroxyshikimic acid in the active site of *Mt*-SK after 7 ns of simulation. The enzyme geometries found in this complex were used for docking studies. Relevant side chain residues are shown and labeled. Significant changes were not observed in the ADP/ATP binding site.

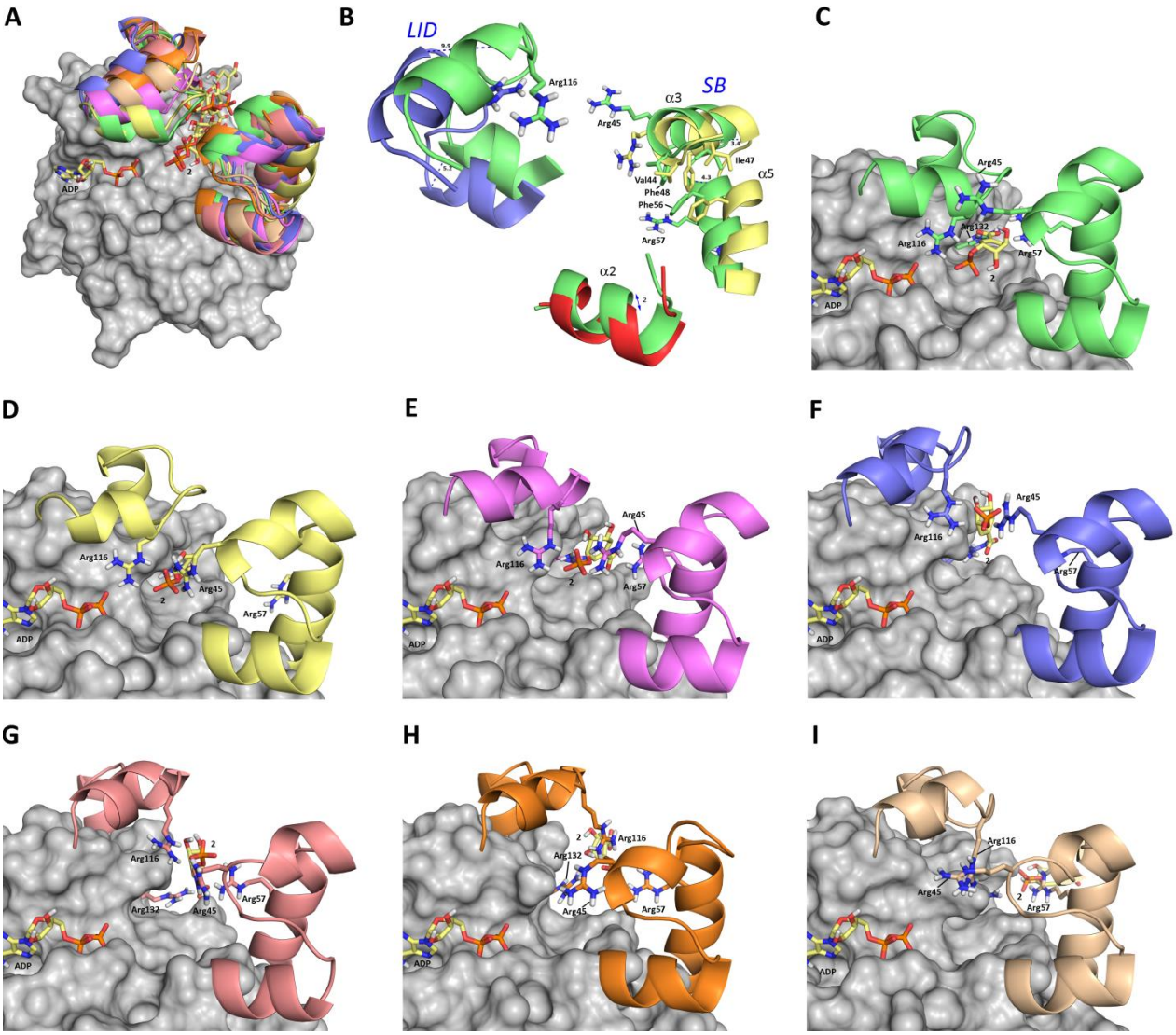

Figure 5. Representative snapshots of product release from the active site of *Hp*-SK obtained by MD simulations. The large conformational changes of the LID and the α-helices α3, α2 and α5 of the SB binding domains during 50 ns of simulation are highlighted. Significant changes were not observed in the ADP binding site. (A) Overall view of the enzyme motion. Superposition of shapshots C–I. (B) Detail of the largest conformational changes observed of the LID and α-helices α3, α2 and α5. (C) After 10 ns. (D) After 23 ns. (E) After 25 ns. (F) After 28 ns. (G) After 32 ns. (H) After 50 ns. Relevant side chain residues are shown and labeled.

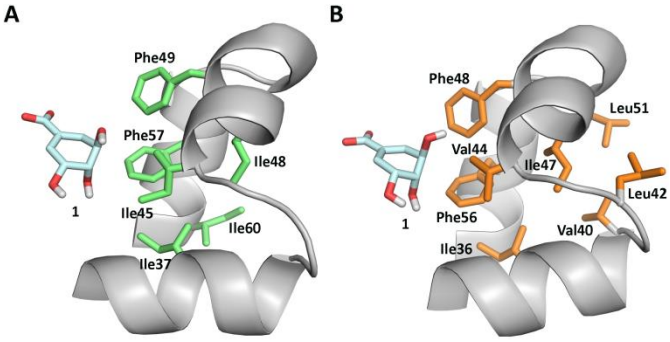

Figure 6. Detail of the apolar pocket in the SB binding domain of *Mt*-SK (A) and *Hp*-SK (B) enzymes. The substrate (cyan) and relevant side chain residues are shown and labeled.

Scheme 2. Synthesis of compounds **3**.[a]

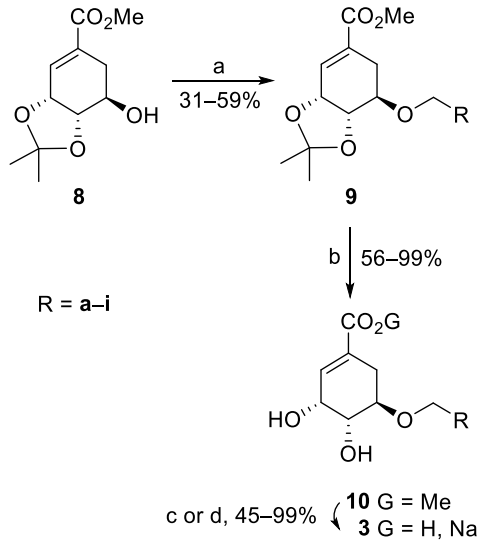

[a]*Reagents and conditions*: (a) RCH_2Br, NaI, DIPEA, 150 ºC. (b) HCl (6 M), EtOH, 60 ºC. (c) 1. LiOH, THF, RT. 2. Amberlite IR-120 (H^+). (d) NaOH, THF, RT. Compounds **3f** and **3d** were obtained directly by acid hydrolysis (b) of **9f** and **9d**, respectively.

Scheme 3. Synthesis of compounds **4–5**.[a]

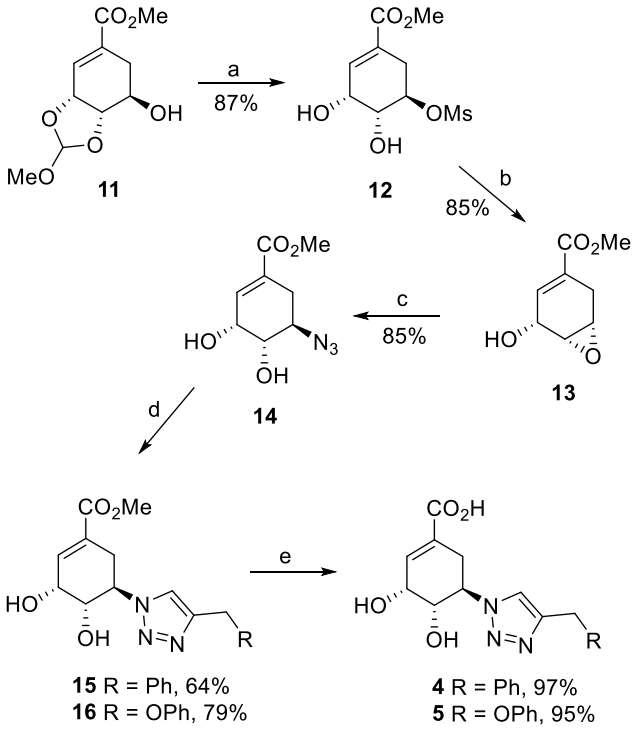

[a]*Reagents and conditions*: (a) 1. MsCl, Et_3N, DCM, 0 ºC to RT. 2. MeOH/H_2O/HCl (100:1:0.1), RT. (b) NaOMe, MeOH, RT. (c) NaN_3, AcOH, 40 ºC. (d) $HCCCH_2R$, sodium ascorbate, *t*BuOH/H_2O, $CuSO_4$, RT. (e) 1. LiOH, THF, RT. 2. Amberlite IR-120 (H^+).

Scheme 4. Synthesis of compounds **6h–i**.[a]

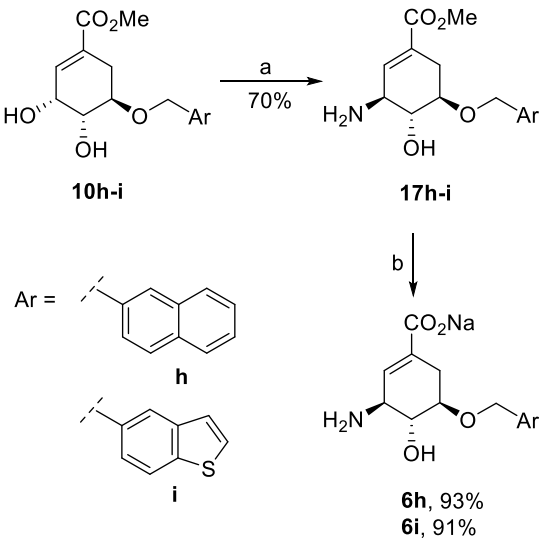

[a]*Reagents and conditions*: (a) 1. HN_3, DIAD, PPh_3, THF, 0 °C. 2. PPh_3, H_2O, THF, Δ. (b) NaOH, THF, RT.

Table 1. K_i (μM) of compounds **3–6** against SK from *M. tuberculosis* and *H. pylori*[a]

Entry	Compound, Ar		*Mt*-SK[b]	*Hp*-SK[c]
1	**3a**	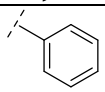	360 ± 14	3.00 ± 0.10
2	**3b**	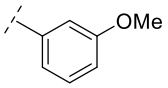	135 ± 5	1.00 ± 0.05
3	**3c**	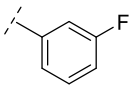	180 ± 5	1.28 ± 0.03
4	**3d**	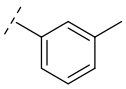	109 ± 5	2.10 ± 0.15
5	**3e**	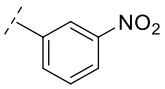	10 ± 1	0.46 ± 0.02
6	**3f**	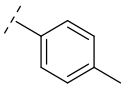	166 ± 16	10.9 ± 0.6
7	**3g**	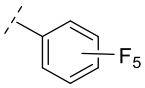	710 ± 50	41 ± 4
8	**3h**	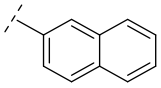	22 ± 1	1.80 ± 0.10
9	**3i**	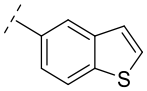	43 ± 1	0.56 ± 0.05
10	**4**	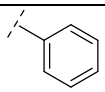	> 2000	95 ± 4
11	**5**	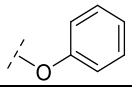	> 2000	67 ± 4
12	**6h**	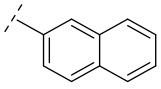	> 2000	> 800
13	**6i**	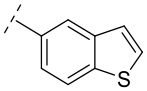	415 ± 21	535 ± 10

[a]Assay conditions: Tris.HCl (100 mM, pH 7.7), ATP (2.5 mM), NADH (0.2 mM), PEP (1 mM), $MgCl_2$ (5 mM), KCl (0.1 M), lactate dehydrogenase (2 units), pyruvate kinase (2.8 units), 25 ºC. [b]K_m (**1**) = 544 μM. [c]K_m (**1**) = 39 μM.

Table 2. The minimum inhibitory concentration (MIC) of methyl esters **10e**, **10i**, **15–16**, **17h-i** against *H. pylori* clinical isolate from Guadalajara Hospital.

Compound	MIC (μg/mL)
10e	128
10i	4
15	256
16	128
17h	64
17i	256
ampicillin	1

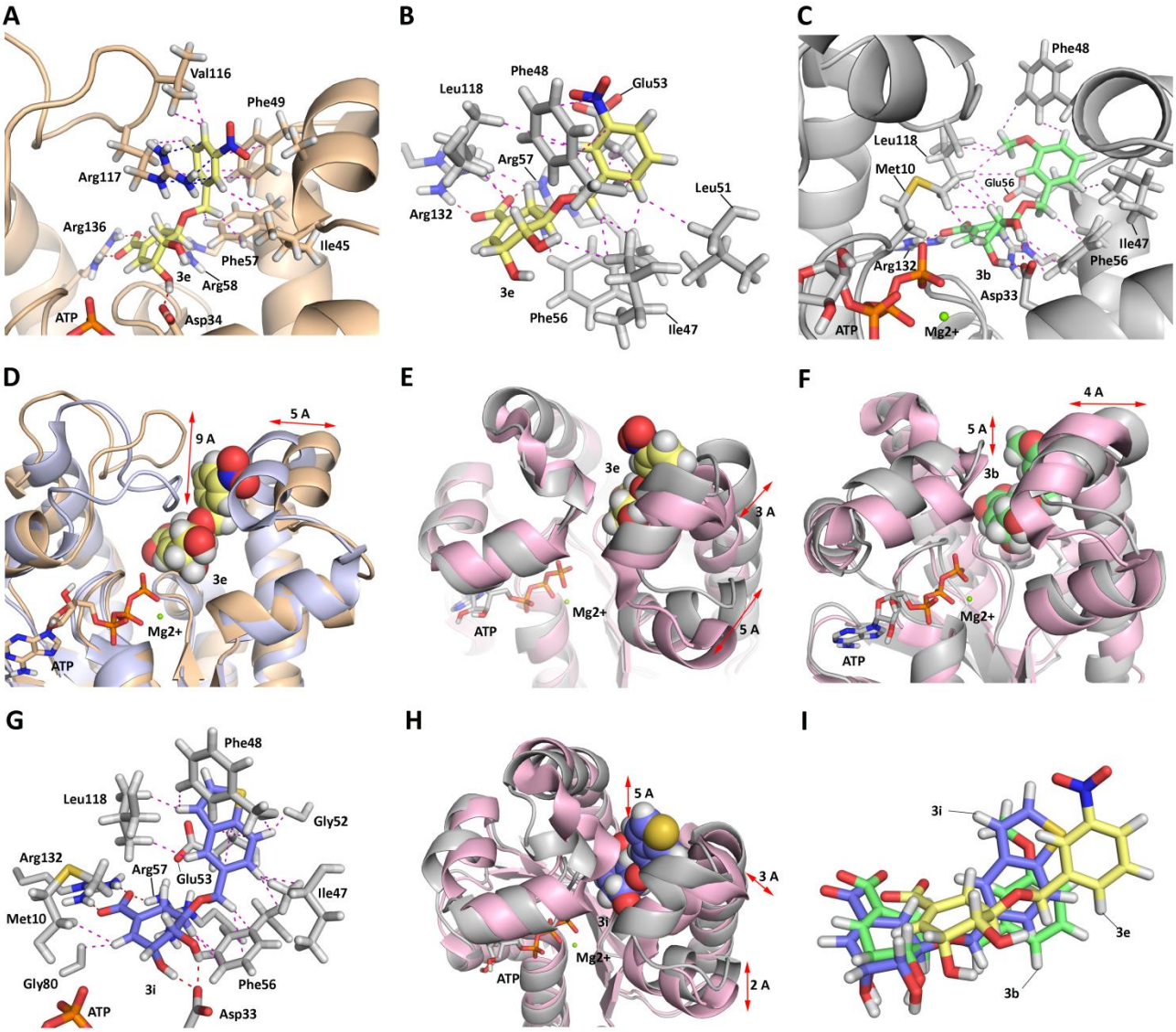

Figure 7. Binding mode of *O*-benzyl derivatives **3e**, **3b** and **3i** obtained by docking and MD simulation studies in the active site of the SK enzymes. (A) **3e** (yellow) in the active site of *Mt*-SK (wheat). (B) **3e** (yellow) in the active site of *Hp*-SK (gray). (C) **3b** (green) in the active site of *Hp*-SK. (G) **3i** (blue) in the active site of *Hp*-SK. (D,E,F,H) Comformational changes in the LID and SB domains of the SK enzymes caused by the binding of compounds **3e**, **3b** and **3i**. The closed active form [PDB codes 2IYQ (*Mt*-SK, D) and 3MUF (*Hp*-SK, E-F and H)] and the inactive arrangement of the SK enzymes are compared for each ligand (spheres). (I) Comparison of the binding mode of compounds **3e**, **3b** and **3i** in the active site of *Hp*-SK. The arrows highlight the most relevant changes

in the LID and SB domains. Relevant side chain residues are shown and labeled. Polar (red) and lipophilic (magenta) interactions between ligands and enzyme residues are shown.

Targeting the Motion of Shikimate Kinase: Development of Competitive Inhibitors that Stabilize an Inactive Open Conformation of the Enzyme

Verónica Prado, Emilio Lence, María Maneiro, Juan C. Vázquez-Ucha, Alejandro Beceiro, Paul Thompson, Alastair R. Hawkins, and Concepción González-Bello*